AD-A280 359

5/11/94 8011

SECURITY CLASSIFICATION

DTIC ELECTE JUN 15 1994 S F D

REPORT DOCUMENTATION PAGE

1a. REPORT SECURITY CLASSIFICATION: UNCLASSIFIED	1b. RESTRICTIVE MARKINGS: N/A
2a. SECURITY CLASSIFICATION AUTHORITY	3. DISTRIBUTION/AVAILABILITY OF REPORT: Approved for public release; distribution unlimited ~~Unrestricted~~
2b. DECLASSIFICATION/DOWNGRADING SCHEDULE	
4. PERFORMING ORGANIZATION REPORT NUMBER(S)	5. MONITORING ORGANIZATION REPORT NUMBER(S): AFOSR-TR- 94 0346
6a. NAME OF PERFORMING ORGANIZATION: Indiana University	6b. OFFICE SYMBOL (If applicable):
6c. ADDRESS (City, State and ZIP Code): 4601 Central Avenue, Columbus IN 47203	7a. NAME OF MONITORING ORGANIZATION: AFOSR/NL
	7b. ADDRESS (City, State and ZIP Code): 110 Duncan Ave Suite B115, Building 410, Bolling AFB DC 20332-6448
8a. NAME OF FUNDING/SPONSORING ORGANIZATION: AFOSR	8b. OFFICE SYMBOL (If applicable): NL
	9. PROCUREMENT INSTRUMENT IDENTIFICATION NUMBER: AFOSR - F49620-93-1-0297DEF
8c. ADDRESS (City, State and ZIP Code): 110 Duncan Ave Suite B115, Building 410, Bolling AFB DC 20332-6448	10. SOURCE OF FUNDING NOS.

PROGRAM ELEMENT NO.	PROJECT NO.	TASK NO.	WORK UNIT NO.
61102F	2312	A5	

11. TITLE (Include Security Classification): Two-dimensional protein pattern recognition in chemical toxicity

12. PERSONAL AUTHOR(S): Frank A. Witzmann, Ph.D.

13a. TYPE OF REPORT	13b. TIME COVERED	14. DATE OF REPORT (Yr., Mo., Day)	15. PAGE COUNT
Annual	FROM 1 Apr 93 TO 30 Mar 94	94 Apr 20	42

16. SUPPLEMENTARY NOTATION

17. COSATI CODES		
FIELD	GROUP	SUB. GR.

18. SUBJECT TERMS (Continue on reverse if necessary and identify by block number): rat liver, rat kidney, rat testis, perfluorcarboxylic acid peroxisome proliferator, 2D protein electrophoresis, image analysis, protein sequence, pattern recognition

19. ABSTRACT (Continue on reverse if necessary and identify by block number)

This report summarizes the progress made in the development of a two-dimensional prot database for toxicity screening and mechanistic determination. Various chemically distinct peroxisome proliferators were compared with regard to their effect on the 2D protein pattern of various target tissues in the rodent. Protein alterations, novel identifications, and future directions are described.

94 6 14 154

94-18490

DTIC QUALITY INSPECTED 8

20. DISTRIBUTION/AVAILABILITY OF ABSTRACT	21. ABSTRACT SECURITY CLASSIFICATION
UNCLASSIFIED/UNLIMITED ☑ SAME AS RPT. ☐ DTIC USERS ☐	unclassified

22a. NAME OF RESPONSIBLE INDIVIDUAL	22b. TELEPHONE NUMBER (Include Area Code)	22c. OFFICE SYMBOL
Dr. Walt Kozumbo	202-767-5021	NL

DD FORM 1473, 83 APR EDITION OF 1 JAN 73 IS OBSOLETE. 10 MAY 1994 SECURITY CLASSIFICATION OF THIS PA

Report AFOSR F49620-93-1-0297DEF

TWO-DIMENSIONAL PROTEIN PATTERN RECOGNITION IN CHEMICAL TOXICITY

Frank A. Witzmann, Ph.D.
Department of Biology
Indiana University-Purdue University at Indianapolis
Columbus Campus
4601 Central Avenue
Columbus IN 47203

20 April 1994

Annual Report for Period 1 Apr 93 through 30 Mar 94

Prepared for:

Dr. Walt Kozumbo
Directorate of Life Sciences
AFOSR
Building 410
Bolling AFB DC 20332-6448

INTRODUCTION

The efforts of this laboratory during the research period have been directed at developing a predictive toxicological approach based on target tissue protein pattern recognition. Through interaction with the Toxicology Division of the Armstrong Laboratory and the unique capabilities we possess, our laboratory has continued the development and expansion of a two-dimensional protein pattern database for each of three rodent target tissues. By using large-scale two-dimensional electrophoresis of proteins (2D-PAGE) combined with computerized image analysis, we have used methods for comparing computer-recognized 2D-protein pattern alterations in various target tissues induced by specific chemical agents. These alterations have been used to indicate and comparatively assess hepatotoxicity, nephrotoxicity, and testicular toxicity by detecting specific patterns of protein alteration.

The effectiveness of the large-scale 2D-PAGE technique used in this laboratory results from the resolution of (in the case of the rat liver) nearly 1,500 cellular proteins in a single sample, first based on their content of acidic and basic amino acids (isoelectric focusing) and second by molecular weight (SDS electrophoresis)(Andersen *et al.*, 1981; George and Andersen, 1986; Olson and Andersen, 1983). In combination, these two separation techniques produce a two dimensional protein pattern unique for each tissue or group of cells tested. Individual proteins within the pattern can be analyzed for alterations in volume (density), charge, and molecular weight. Changes in volume or spot density reflect alterations in a protein's abundance and suggest up- or down-regulation of the genome or altered protein turnover rates. Charge modifications suggest either posttranslational modification such as phosphorylation, ribosylation, conjugation or amino acid substitutions resulting from point mutations in the genome.

Regardless of the type of changes observed, a well-resolved 2D protein pattern, or 2D protein map (fingerprint), provides a pattern realistically containing 1000-2000 proteins and is thus a significant source of information regarding the health/activity of a particular cell/tissue type and its response to toxic insult. With the application of computerized imaging of the protein patterns generated by 2D-PAGE, its use in pattern recognition for animal model target tissues, and the recent advent of microsequencing proteins isolated from 2D gel patterns (Hughes *et al.*, 1992), 2D-PAGE has become an even more powerful technique in toxicity testing; one with increasingly well-documented potential (Anderson, 1990). For example, Hochstrasser *et al.* (1992) have reviewed the clinical (diagnostic) applications of high resolution, large-scale 2D electrophoresis and its use in the clinical analysis of human body fluids, blood cells, and various tissues. Correspondingly, the long-term objective of the present investigation is to generate a 2D protein database for toxicologic targets, one that can be used to analyze chemical effects both in vivo and in vitro.

This report details the progress made during the research period 1 April 1993 to 30 March 1994 in each of the following areas:

- O Perfluorocarboxylic acid toxicology (comparative peroxisome proliferator toxicity) - pattern alterations in 2D protein maps
- O Database Development
  - -identification of proteins via peptide mass fingerprinting
  - -MW estimation and standardization of master-pattern based on amino acid composition
  - -isoelectric point estimation and standardization of master-pattern based on amino acid composition
  - -inclusion of normal average abundances for each protein in the database
  - -construction of rodent kidney and testis whole homogenate protein databases
- O Improved resolution of all sample proteins with pI > 7.0 via first-dimension immobilized pH gradient electrophoresis (IPG-DALT)

MATERIALS AND METHODS

Animal Care and Intoxication. Male Fisher-344 rats (225-250g) were obtained from Charles River Breeding Labs, individually housed, and maintained on rat chow and water ad libitum. PFDA and PFOA, Aldrich Chemical Company (Milwaukee WI), were dissolved in propylene glycol and water, 1:1 by volume, and concentration adjusted so that the dose volume did not exceed 0.5 ml. Rats were injected intraperitoneally with the above solutions so that exposures were as follows: 2 mg (n=5), 20 mg (n=5), and 50 mg PFDA/kg body weight (n=9), single injection, animals sacrificed on day 8 of exposure; 50 mg PFDA/kg body weight (n=5), single injection, 30 days after exposure; and 150 mg PFOA/kg body weight (n=8), single injection, animals sacrificed on day 3 of exposure. Clofibrate (ethyl-α-p-chlorophenoxy-isobutyrate), Sigma Chemical Co. (St. Louis MO), was administered as neat oil, 250 mg clofibrate/kg body weight, single intraperitoneal injection on each of 3 successive days, animals sacrificed on day five of exposure (n=10). DEHP, Aldrich Chemical Company (Milwaukee WI), was administered as neat oil via oral lavage, 1200 mg/kg per day, animals sacrificed on day 5 of exposure (n=3). Matched control rats were vehicle injected and pair fed (PFC; n=10) while one group (Ad Lib; n=6) served as free-eating controls. It is important to emphasize that the route and level of toxicant exposures described above have previously been shown to result in maximal peroxisome proliferation with minimal lethality in male rats (Okita *et al.*, 1993; George and Andersen, 1986).

Sample Preparation. After each exposure period, livers were surgically removed from the ketamine/xylazine anesthetized rats and manually perfused with ice-cold saline to remove excess blood. One 0.5g piece was removed, minced, and homogenized in 8 volumes (4mL) of a lysis buffer containing 9M urea, 4% NP-40, 2% DTE (dithioerythritol), and 2% ampholytes (Serva pH 9-11) pH 9.5 for ISO-DALT® electrophoresis (Anderson, 1988). After solubilization at room temperature for 120min, all samples were centrifuged at 100,000 x g for 30 min using a Beckman TL-100 ultracentrifuge to remove insoluble materials and nucleic acid and the supernates stored at -70°C. A second liver sample was removed from some PFDA-treated rats, homogenized in ice-cold 0.25M sucrose, and the microsomal fraction prepared by differential centrifugation (Tata, 1972). This fraction was then solubilized in lysis buffer, centrifuged, and stored as described above.

Two-dimensional Electrophoresis. Using the Anderson ISO-DALT® (2D Electrophoresis) System (Anderson, 1988), 8-10 µl of the solubilized protein sample was placed on each of 20 first dimension gels (25 cm x 1.5 mm) containing 4% acrylamide (Protogel from National Diagnostics, Atlanta GA), 9M urea (BDH), 2% NP-40, 2% ampholyte (BDH pH 4-8) and electrophoresed for 32,000 VHr at room temperature. Each first dimension gel was then placed on a second-dimension DALT slab gel (20 cm x 25 cm x 1.5 mm) containing a linear 11-17% acrylamide gradient. Gradient slab gels were poured reproducibly using the ANGELIQUE™ computer-controlled gradient maker (Large Scale Biology Corp.). This system reduces run-to-run variability in the polyacrylamide gel concentration, an essential characteristic for protein pattern image analysis. Molecular weight standards (Sigma) were comigrated on the gel margin while internal charge standardization was accomplished using carbamylated creatine kinase charge-train standards obtained from Pharmacia (Piscataway NJ). DALT gels were run for approximately 18 hr at 150 V and 10 C and later stained with Coomassie brilliant blue G-250 (Bio-Rad)(Neuhoff *et al.*, 1988).

Protein patterns on replicate gels were electroblotted for immunological identification of Grp78/BiP and Hsp60. Proteins were transferred onto PVDF membranes (Millipore) (in 49mM tris - 39mM glycine buffer with 0.04%SDS and 20% methanol, pH 9.2) using the Bio-Rad Trans-Blot Semi-Dry transfer cell for 37.5 VHr at room temperature. The membranes were washed and blocked with several exchanges of 2.5% powdered milk in PBS (0.15M NaCl, 0.05M phosphate buffer, pH 7.2) and incubated with primary antibody (1:1000 in PBS with 0.1% w/v bovine serum albumin): either rabbit anti-Grp78/BiP (StressGen, Victoria BC Canada), which recognizes only Grp78/BiP in murine, rat, and hamster cell lines, or anti-hsp60 (StressGen).

Identification of Grp78/BiP was confirmed by comigration of recombinant hamster Grp78 (StressGen). The 2D coordinate position of Grp78/BiP relative to other proteins in the rat liver whole homogenate pattern has previously been established (Witzmann *et al.*, 1994b) using methods identical to those described here. Blots were then washed with 0.1% powdered milk in PBS, incubated with goat anti-rabbit peroxidase conjugated IgG, and visualized using 4-chloronaphthol. Other stress proteins mentioned later in this report were identified by similar methods using StressGen antibodies and purified proteins.

Image Analysis. Stained gels and wet protein blot membranes were digitized at 125 micron resolution using an Ektron 1412 CCD scanner that produces 8 bit images in the optical density domain with up to 2048x2048 pixels although most images were 1838x1966 pixels. The gel images were processed on a DEC VAXStation 3100/76 workstation using the KEPLER® software system (Large Scale Biology Corp.) with procedure PROC008. This procedure uses background and streak subtraction, erosion/dilation spot cutout, and 2D Gaussian fitting to generate a spotlist giving x,y position, shape, and density information for each detected spot. Groups of numerous sample gels corresponding to all the animal treatment groups were assembled and matched to a standard master pattern F344LIVER_1 (Figure 1) for this particular experiment and set of running conditions. Individual gel patterns were scaled using a linear fit to the abundances of 389 selected spots to compensate for variations in sample protein loading as previously described (Anderson *et al.*, 1987). In effect, 389 protein spots (whose volume, shape, presence in each pattern, and coefficient of variation are consistent and occur in a narrow range of values throughout the experimental group patterns) were chosen and scaling factors for each pattern calculated prior to statistical comparison of the individual spots. Groupwise statistical comparisons (Student's t-Test) were made graphically and interactively and the results displayed in montage format using the KPL42 module. Graphical results of individual spot statistics and spot maps were printed in postscript on a microLaser Plus printer (Texas Instr.) while raw gel images and spot profiles were printed using a 64 level grey-scale videoprinter (Codonics). Spot volume information generated by Kepler™ was exported to a PC (Gateway2000) for one-way ANOVA and the SNK multiple comparison test using SigmaStat (Jandel).

The level of charge modification was determined by calculating the Charge Modification Index (CMI) (Anderson *et al.*,1992) for each sample. This index describes the overall average number of charges added per protein molecule examined. Table 1 illustrates the CMI calculation of Grp78/BiP for a

Table 1. Charge Modification Index

Grp78/BiP charge variants	MSN 1537	MSN 1536	MSN 18	MSN 14	MSN 5	TOTAL
Protein Abundance (A)	1,048	2,153	22,000	39,300	82,600	147,101
Charge (C)	-4	-3	-2	-1	0	
Protein Charge, (A x C)	-4,192	-6,459	-44,000	-39,300	0	-93,951

Charge Modification Index (CMI) = Total Charges/Total Protein
= -93,951/147,101
= -0.64

representative sample from the pair-fed control group; an identical calculation was conducted for Grp78/BiP and Hsp60 in each sample and the group means compared by one-way ANOVA as mentioned above and is presented in the results section on page 8.

Peptide-mass Fingerprinting. Protein identification via sequencing of peptides has traditionally been done via Edman chemistry. This process is requires tens of picomoles of purified sample and does not function well when analyzing proteins with either modified or unusual amino acids or those that have a blocked N-terminus. Recent developments in the time-of-flight mass spectrometry (TOF-MS) of matrix-assisted laser desorption/ionization (MALDI) allow accurate molecular mass determination of the peptide products of proteolytic cleavage. Sub-picomole amounts of a protein can now be proteolytically digested and the masses of the peptide products accurately determined. The results of such proteolytic cleavages and peptide mass determinations can be compared to a database of peptide masses and identified, provided the protein has been sequenced and is in the database. We applied this innovative technology to proteins separated by 2D-PAGE in an effort to determine its efficacy with regard to our need for rapid yet accurate methods for identifying the hundreds of proteins resolved in our electrophoretic system. In doing so, we assumed that proteins on 2D gels are significantly pure and can be isolated and digested to yield constitutive peptides that can be isolated, masses determined and submitted to the MOlecular Weight SEarch (MOWSE) (Pappin *et al.* 1993) database for identification.

Tryptic digestion *in situ*. Various protein spots with known identity (cytochrome b_5, superoxide dismutase, and FABP-L) were cut from each of 11 replicate 2D gels along with 11 blank acrylamide cutouts. These cutouts were destained overnight in 50% methanol, washed with H_2O several times, weighed, and air-dried for 2hrs. Using a scalpel blade, the 11 acrylamide cutouts for each protein and blank were cut into fine pieces (<1mm^2) and rehydrated with a trypsin solution (2µg modified trypsin (PROMEGA) in 300µl 25mM NH_4HCO_3 buffer pH 7.8) in which the estimated [E]:[S] was approximately 1:50. Digestion was conducted in closed microcentrifuge tubes for 24hr at 37°C. Peptides were eluted from the digest with 2 X 750µl washes using 60% acctonitrile/0.1% trifluoroacetic acid and intermittent vortexing. Following brief centrifugation (13,000 x *g*), the 1.5ml eluent was speed-vacuumed to dryness and peptides resuspended with 60% acetonitrile.

Tryptic digestion of hydrophobic (Immobilon-P) PVDF-bound proteins. Proteins resolved on stained or unstained 2D gels were electroblotted onto either Immobilon-P or Immobilon-CD PVDF membranes (Millipore Corp.) using conventional western blotting techniques. Known protein spots were cutout, destained with 70% acetonitrile (1ml/spot), air-dried, and cut into small 1-2mm pieces. The membrane pieces were placed in a 0.5ml Eppendorf tube and 2-4µl of working incubation buffer was added (25mM NH_4HCO_3, 1% octyl glucoside, 10% methanol, 5mM dithiothreitol, and modified trypsin [20µg/ml;] to give an approximate [E]:[S] of 1:10). After the digests incubated for 18hr at 37°C, 10µl of ethanol was added to the tube to elute the peptides for 1hr. The tubes were centrifuged for 15 minutes at 13,000 x *g*, and the supernate collected. The wash and centrifugation were repeated using 50% ethanol and the supernate collected. The supernates were pooled, lyophilized, and the peptides resuspended in 2-4µl of 10% methanol.

Tryptic digestion of cationically derivatized (Immobilon-CD) PVDF-bound proteins. PVDF-CD blots from unstained gels were reverse-stained, selected protein spots cut-out, and cut into 1-2mm pieces. Immobilon-CD was used because its cationic surface allows easier recovery of blotted proteins/peptides. The membrane pieces were placed in a 0.5ml Eppendorf tube and 4µl of working incubation buffer was added (25mM NH_4HCO_3, 1% octyl glucoside, 5mM dithiothreitol, and modified trypsin [40µg/ml;] to give an approximate [E]:[S] of 1:10), some incubated at room temperature, some at 37°C. Following digestion, peptides were eluted with 10-20µl of 50% formic acid in ethanol (v/v) for 1hr and saved for mass spec analysis.

Matrix-assisted laser-desorption/ionization mass spectrometry of peptides (MALDI). Using the Finnegan Lasermat® laser-desorption mass spectrometer (located at Large Scale Biology Corp., Rockville MD), the peptide masses eluted from the above protein digests were determined and analyzed. In this instrument, sample ions are generated by UV laser bombardment as a result of proton transfer from matrix to the peptides. These sample ions are accelerated in an electric field and drift through a field-free

region to a detector. The mass of each ion can be calculated based on its time of flight, *i.e.* the time it takes to reach the detector. With a sensitive detector and an efficient ionization technique, it is generally accepted that proteins and especially peptides with molecular masses <100kD are readily desorbed/ionized by MALDI and masses accurately determined (Arnott *et al.*., 1993). 0.5µl aliquots of the tryptic digests described above were placed on a stainless steel target along with 0.5µl of either 100mM sinapinic or 33mM α-cyano-4-hydroxy cinnamic acid and the target was air-dried. Data was collected and detected masses were displayed and archived as both hardcopy output and PC file storage. Known protein masses were submitted to the MOWSE database and compared to peptide mass fingerprints generated from the Swiss-Prot, Protein Identification Resource, and GenBank databases.

Estimation of pI and MW. Isoelectric point was calculated based on amino acid composition (Neidhardt *et al.*, 1989; Anderson *et al.*, 1991). To standardize the rat liver 2D protein map, pI was calculated for the proteins we have conclusively identified and whose sequence is known (PIR/SWISS-PROT, DB Release 35). These included calmodulin (pI 3.85) to catalase (pI 7.45) as well as 20 others with pIs distributed within that range . Using these pIs with their corresponding *x* coordinates, a standard fitted curve was calculated using Tablecurve Software (Jandel). The pI estimate for each protein in the database was then calculated based on this equation. A similar method was applied to molecular weight estimation. The same proteins used in pI estimation were used to calculate MW. The identified protein MW was obtained directly from the PIR/SWISS-PROT databases where it is calculated from amino acid composition. As before, a standard fitting curve was calculated from MW and *y* coordinate data. Because we use an 11-17% acrylamide gel gradient for 2nd dimension separation, the fitting curve was not limited by some predetermined model. Rather, we selected the equation that described a curve that best fit the data from the many generated by Tablecurve. The *y* coordinate data from each protein in the database was then used to estimate MW.

RESULTS AND DISCUSSION

Peroxisome Proliferator Studies - BiP/Grp78 and Hsp60. With the exception of Tables 1 and 2, all data are compiled in the Addendum. Figure 1 illustrates the master pattern F344LIVER_1, in which the standard 2D pattern of over 1,400 whole homogenate proteins is displayed. This master pattern is essentially a composite of all proteins detectable in the 61 samples that comprise this experiment and serves as a reference for comparison of current and future experimental rat liver protein patterns generated under similar running conditions. Each circle or ellipse represents either a distinct protein or alternate forms of the same protein. Each protein spot is also arbitrarily assigned a master spot number (MSN) connoting that protein's identity in the database for F344LIVER. Although many proteins in this pattern are altered by the chemical treatments described, this report focuses on BiP/Grp78 (Fig. 1, upper left) and Hsp60 (below, right), whose identities and appearance as trains of charge variants were confirmed immunologically and by comigration of purified BiP/Grp78. In this electrophoretic system, proteins that ordinarily exist as "microheterogeneities" are assumed to have undergone some form of post-translational modification such as phosphorylation, glycosylation, deamidation/amidation or conjugation. These microheterogeneities are observed as trains of spots with similar molecular weight trailing to the left (acidic) end of the slab. Typically, the most basic component of this "charge train" is the "parent" or unmodified form. This unique feature of the 2D pattern is especially conspicuous in serum protein patterns (Anderson and Anderson, 1991) where glycosylated proteins are numerous.

While the master pattern in Figure 1 shows 5 distinct Grp78/BiP charge variants, only those 3 with the most basic pI are normally expressed in the untreated liver. The additional 2 acidic charge variants of Grp78 have been observed almost exclusively in PFDA-treated rats. Hsp60 normally appears as the three spots shown on the master pattern; no additional charge variants (neither acidic nor basic) have been

observed in our experiments.

Modifications induced by PFDA exposure (50mg/kg, 8da) are illustrated by representative gel-patterns in Figure 2A & B. In the pair-fed control protein pattern (Fig. 2A), Grp78/BiP exists as three and a minor fourth charge variants. In contrast, a typical pattern representing the PFDA (50mg/kg, 8da) treatment group is also shown (Fig. 2B). This 2D pattern shows a distinct leftward shift in protein abundance, from the most basic parent species to more acidic forms. Other treatment groups failed to exhibit this obvious shift and are therefore not shown. In contrast to Grp78/BiP, Hsp60 appears to undergo a proportional induction of all charge variants as a result of PFDA exposure and not a specific acidic charge-shift. Total protein abundance of Grp78/BiP across the experimental groups (calculated by summing the individual abundances of all charge forms) was slightly increased by the PFDA (50mg/kg, 8da) exposure only ($F=4.11$, $p<.001$), while all experimental manipulations, with the exception of PFDA (2mk/kg), caused a significant induction of total Hsp60 abundance ($F=15.52$, $P<.001$). Hsp60 was thus chosen to reflect a protein quantitatively altered by chemical exposure in distinct contrast to the qualitative alterations detected in Grp78/BiP.

The comparison of all treatment groups regarding abundance of charge variants per group is shown in Figure 3. The calculation of charge relative to the major, native form was based on the internal charge standardization described above and analogous to that performed previously (Anderson, 1992). Based on this standardization, native BiP/Grp78 has an apparent pI of approximately 4.84. In the case of PFDA, BiP was clearly and significantly modified by the addition of negative charges rendering the charge variants more acidic and reducing the abundance of the major, native form. Furthermore, this modification persisted virtually undiminished at 30 days following the single exposure. PFDA also had a minor effect in this regard at lower exposures (2 and 20mg/kg) as did PFOA. In comparison, the classic peroxisome proliferators clofibrate and DEHP exerted less effect in this regard.

To determine the quantitative effect of the exposures on total BiP/Grp78 abundance, the sum of all charge variants per gel pattern was calculated, statistical comparisons made, and the results illustrated in Figure 4. Significant differences ($F=4.111$, $p<.001$) were observed between the following: PFDA (50mg/kg, 8 da) vs. PFDA (2mg/kg), Ad lib, and clofibrate and PFDA (50mg/kg, 30 da) vs. PFDA (2mg/kg).

Microsomal patterns from control (MICROSOME_1), PFDA-treated (50mg/kg; 8 (L003E), halothane ($CF_3CHClBr$) hepatitis (L003H), and a protein blot exposed to anti-TFA serum (L003I) are illustrated in Figure 5. This figure documents the identity of the trifluoroacetylated ER 80kDa protein from halothane-exposed rats with BiP/Grp78 (arrows). The major protein to the lower-left of BiP has recently been identified (unpublished) as protein disulfide isomerase (PDI)(double arrow). Due to its partial sequence homology with BiP and its own trifluoroacetylation (Martin et al., 1989), it is also weakly recognized by the anti-TFA serum in pattern L003I.

A comparison of the CMI from all treatment groups is shown in Table 2 (next page). Based on this calculation, 8 day exposure to PFDA (50mg/kg) was associated with a significant modification of Grp78/BiP by the addition of negative charges. Furthermore, this modification persisted virtually undiminished at 30 days following the single exposure. PFDA also had a lesser, statistically insignificant effect at 20mg/kg as did PFOA. Comparatively, clofibrate did not significantly alter CMI although the minor elevation (0.21) resembled that associated with PFOA (0.17), while DEHP exerted no effect whatsoever. With regard to Hsp60, Table 2 confirms the lack of charge modification of this protein shown in Fig. 2. In fact, none of the treatments elicited a change in Hsp60 CMI greater than 0.17.

This segment of the investigation evaluated the alterations in rat liver whole-homogenate 2D protein patterns associated with a group of structurally diverse peroxisome proliferators as indicators of specific *in vivo* effects. Specifically, attention has been focused on the calculable, as well as visible, charge modifications induced exclusively in the endoplasmic reticular protein Grp78/BiP by a perfluorocarboxylic acid (PFDA) and those noticeably absent from another well known stress protein, Hsp60.

The statistically significant alteration in the small population of charge variants of Grp78/BiP

associated only with high-dose PFDA exposure and the induction of aggregate Grp78/BiP supports the view that, while PFDA is a potent peroxisome proliferator (PP), its mechanism may be very different from that of classic PP's like clofibrate and DEHP. To interpret the meaning of the observed protein modifications and how PFDA's toxic mechanism may be different, one must consider BiP's normal cellular function. As mentioned earlier, BiP is believed to be involved in the processing of secretory proteins and the recognition, retention and degradation of misfolded or misassembled proteins in the ER. In carrying out this function, BiP is phosphorylated (Hendershot *et al.*, 1988) and ADP ribosylated (Leno and Ledford, 1990). It is also known that both phosphorylation and ribosylation are associated with nonfunctional or inactive BiP (Hendershot *et al.*, 1988; Leustek *et al.*, 1992). Thus the cell may regulate its protein secretory activity not necessarily by synthesizing more or less BiP but rather by post-translational modification of existing protein. Since the dephosphoprotein and deribosylated forms are the active forms, our observations of leftward, acidic shifts from the native, most basic charge form of BiP suggest that PFDA may cause the inactivation of BiP despite increasing its abundance. This assumes that the observations are indeed ribosylation, phosphorylation, or both.

Table 2. Charge Modification Index (CMI) of Grp78/BiP and Hsp60

Treatment	n	Grp78/BiP CMI	Grp78/BiP Treatment - PFC	Hsp60 CMI	Hsp60 Treatment -PFC
Pair-fed Control (PFC)	6	-0.65	NA	-0.49	NA
Ad lib fed Control	9	-0.62	0.03	-0.34	0.15
PFOA (150mg/kg)	8	-0.82	0.17	-0.32	0.17
PFDA (2mg/kg)	5	-0.75	0.1	-0.41	0.08
PFDA (20mg/kg)	5	-0.96	0.31	-0.46	0.03
PFDA (50mg/kg; 8da)	9	-1.3*	0.65*	-0.4	0.09
PFDA (50mg/kg;30da)	5	-1.36*	0.71*	-0.45	0.04
Clofibrate	10	-0.86	0.21	-0.45	0.04
DEHP	3	-0.61	0.04	-0.43	0.06

Values shown above are group means; comparisons were made via one-way ANOVA (Grp78/BiP, *F=12.638, $p<0.001$; Hsp60, F=3.433, n.s.). Pairwise multiple comparisons of Grp78 by Student-Newman-Keuls method ($p<0.05$) revealed that PFDA exposures, 50mg/kg, (8da and 30da) differed significantly from all other groups but not from each other. No other significant differences were observed.

It is unlikely that the present alterations are the result of adduct formation such as the methapyrilene effects observed previously in F344 rat liver (Anderson *et al.*, 1992) and *in vitro* (Richardson, *et al.*, 1993). In those studies, methapyrilene-protein conjugation resulted in the appearance of as many as 6 additional charge variants of Hsp60 and a change in CMI of over 1.00 (-0.42 to -1.52). Regarding Grp78/BiP in the present study, a large number of new charge variants do not appear as a result of PFDA intoxication. Instead,

an increase in the abundance of those occurring naturally and a significant decline in the abundance of the "parent" form occurs. This decline results in a comparatively modest elevation in CMI of 0.65-0.71 (-0.65 to -1.30 or -1.36), an acidic shift more representative of enhanced ribosylation or phosphorylation effects. That this PFDA-induced effect should persist even 30 days after single-dose exposure relates to the inability of the liver to metabolize PFDA (Vanden Heuvel *et al.*, 1991a and b) and that PFDA accumulates there more than in any other tissue (George and Andersen, 1986).

Whether this peculiar PFDA effect on Grp78/BiP is *1)* a part of a generalized stress response (i.e. oxidative stress), as suggested by the induction of total Hsp60, that results in elevated phosphorylation or (ribosylation) of BiP to stop the export of certain proteins from the hepatic ER or *2)* a specific, primary effect attributable to PFDA intoxication is being studied and will be the subject of a pending report. Nevertheless, PFDA exposure results in distinctive changes in this important cellular protein in direct contrast to the other PP's studied. These data also demonstrate that one need not necessarily look for a increase or decrease in the abundance of stress proteins such as those seen here and in other studies, but rather one can observe subtle qualitative changes that cannot be detected easily via other means.

Although PFDA's specific mechanism and peroxisome proliferative mechanisms in general have not been elucidated from these data, this study has confirmed our expectation that high-resolution 2D electrophoresis in combination with image analysis can reveal subtle biochemical changes associated with important xenobiotic effects. As more proteins are identified in our database of rat liver 2D patterns and those of others, it will be possible to assess enzyme induction, modification, and protein conjugation and to explore cellular metabolic pathways associated with specific intoxications (*i.e.* peroxisomal β-oxidation).

The data presented conform to the criteria established for systematic use of 2D electrophoresis in toxicology (Anderson, 1990) in that we have detected a reproducible effect that is characterized by detectable changes at the molecular level, changes that are specifically associated with a molecular effect that enables one to differentiate various classes of mechanisms. Further investigation, already underway, will ensure that there is a firm basis for expecting that the molecular changes can be interpreted in a way that helps explain not only the details, but also the significance of the events observed.

Peroxisome Proliferator Studies - other proteins not previously reported.

Stress Proteins. Various members of the heat-shock and glucose-regulated protein families have been identified in our rat liver protein database and their 2D coordinate positions are illustrated in Figures 6 and 7. Stress protein regulation in response to peroxisome proliferator exposure is of particular interest because these proteins serve as reliable biomarkers of cell and tissue damage. Secondly, they represent a group of proteins whose abundance and qualitative characteristics tend to vary as a group (*i.e.* pattern alteration) and can be used to demonstrate the specific compartmental effects of xenobiotics. The effect of exposure to PFDA, PFOA, clofibrate and DEHP on these proteins is shown in Figures 8 and 9A-E. In these figures each bar represents an experimental sample. Groups of bars are separared by thin vertical lines. The leftmost group is Ad Lib, second is Pair-fed, and so on. Induction of total Hsp60 and Grp78/BiP by PFDA (50mg/kg, 8da, *i.e.* the sixth group) already has been described. It also appears that up-regulation of stress-proteins occurs only in Grp78/BiP, Hsp60, and Grp75 in response to LD50 exposure to PFDA. Clofibrate and DEHP, both at peroxisome proliferative exposure levels, exhibited little or no stress protein induction. While this may be a poor group of proteins to use as an indicator of a generalized stress response, the observations do suggest that structurally diverse PP's have very different secondary effects, some related to a generalized stress effect and others not.

Senescence Marker Protein-30 (SMP30). MSN 62 (and a charge variant MSN 141) was identified as SMP30 via N-terminal amino acid sequencing on our master pattern. SMP30 is a soluble protein found predominantly in the liver and kidney of male rats, is widely conserved among higher animals, and decreases androgen-independently with aging. Its reported MW (33,387) and pI (4.9) (Fujita *et al.*, 1992) are in close

agreement with our estimates MW 35,560 and pI 4.97. This novel protein has been suggested to have a significant regulatory function manifested by changes in concentrations. Although its specific role is uncertain, it may have hydroxysteroid sulfotransferase activity. Figure 10 illustrates a 2D map of the proteins in our database that have been identified thus far. MSN 62, SMP30 located just below and to the left of β and γ actin, is significantly down-regulated by PFOA, PFDA (at 20mg/kg >), and clofibrate (Fig. 11 & 12). DEHP results in a less significant reduction (attributable to the small *n*). Although the significance of this down-regulation is not yet clear, SMP30 may prove to be an excellent biomarker for this type of intoxication.

Alpha 2u Globulin (α2u). Another protein significantly altered is α2u-globulin. Tentatively identified by homologous position (Large Scale Biology, Corp.), this protein is significantly down-regulated by pair-feeding (essentially food restriction) and nearly undetectable in the PFDA 50mg/kg, 8 or 50da, exposures (Fig. 13). In this respect, clofibrate and DEHP had no significant effect. Alpha 2u-globulin is a 19,000 Da protein with an estimated pI of 5.48. It is produced in the liver of adult male rats under multi-hormonal control, is secreted into the general circulation, and generally declines with age. Circulating α2u-globulin is endocytotically taken up by the kidney and catabolized. Exposure to various xenobiotics, including chlorinated hydrocarbons, results in accumulation of α2u-globulin in the kidney cortex as hyaline droplets, a phenomenon known as "α2u-globulin nephropathy" (Lock, 1993). However, hepatic concentration of α2u-globulin is not altered during such exposures. The reduction observed in α2u-globulin abundance to at-or-below the limits of detection in the male rat liver by PFDA (but not clofibrate nor DEHP) is nearly identical to the effect on α2u-globulin (MSN 110) observed in the kidney (Fig. 14). The down-regulation of α2u-globulin in the liver evidently results in less accumulation in the kidney where its abundance is normally more than ten-fold that in the liver (Lock, 1993). The underlying mechanism of hepatic α2u-globulin's decline is unknown. Nevertheless, the subsequent decline in renal α2u-globulin is likely a function of hepatic events. Interestingly, this effect parallels the alteration observed in hepatic SMP30, another protein whose synthesis is subject to senescence. The involvement of immunoglobulin heavy-chain binding protein (BiP/Grp78) and its possible inactivation by PFDA (Witzmann *et al.*. 1994a & b) in the decrease in α2u-globulin is being investigated. The relationship between these proteins and others with respect to the unique hepatotoxicity of PFDA is also under investigation.

Database Development. Identification of proteins via peptide mass fingerprinting. Our attempts to conclusively identify proteins from 2D gels using MALDI-TOFMS was unsuccessful. Initial efforts using *in vitro* tryptic purified proteins (*i.e.* bovine hemoglobin) followed by mass spec analysis of the peptides and submission of these data to the MOWSE database demonstrated that this approach provided excellent peptide mass accuracy (Fig. 15). This figure illustrates the peptide masses obtained by tryptically digesting bovine hemoglobin (actually a mixture of α and β chains) as described in the methods section. Results of the peptide mass search (Addendum B) show that out of 30 "hits", α chain was number 1 while β chain was fifth. The last two pages show the peptides that actually matched. When the digestion was attempted on various protein spots in acrylamide cutouts, results like those in Figure 16 were obtained. This figure illustrates a mass spectrum of cytochrome b_5 digest. While masses were certainly detected, confirming trypsin proteolysis, the masses were inaccurate with regard to those expected for cyt b_5. Repeatedly, this and other known proteins gave spurious results. We concluded that residual SDS and acrylic acid co-eluted from the sample digest interfered ionization of the sample-matrix mixture on the mass spec target, thus quenching the signal and yielding inaccurate masses. Passing the eluted peptides through a hydrophobic C4 column and eluting them from the column resulted in little improvement. Conducting digests on proteins blotted onto PVDF membranes gave slightly better results although there was little difference between these and the results in Figure 16. Because of logistical considerations in conducting these experiments at LSB Corp. in Maryland and the intended scope of the project reported here, we have mutually decided not to pursue these studies further.

MW and pI Estimates; standardization of the database. Figures 17 and 18 illustrate the fitting curves and the equations for those curves used in calculating the estimated MW and pI for each protein in the rat liver 2D protein database. As a result, each of the protein spots on the master pattern for liver was given an estimated pI and MW. Table 3 shows a sample of the database, listing the proteins we currently identify (either confirmed or tentative). Our estimates are in excellent agreement with other rodent liver databases and published individual protein data. While we acknowledge that these data are only estimates, the MW and pI values will be used to improve the identification of unknown protein spots by enabling us to identify probable gel locations and "narrow the playing field." The table also includes a data column listing the average "normal" abundance for a specific protein spot obtained under the standardized running conditions. This information will also be useful to screen probable spots for identification. In identifying the 2D location of proteins known to exist in large abundance in the liver, those spots with very low abundance situated in the probable gel coordinate location can thus be eliminated from consideration, and *vice versa*.

Construction of rodent kidney and testis whole homogenate protein databases. Figures 19 and 20 illustrate the rat kidney whole homogenate 2D master pattern (F344KIDNEY_1) and the rat testis whole homogenate 2D master pattern (F344TESTIS_1), respectively. These data have been generated using tissues obtained from the identical animals that provided the liver samples. The 2D gels were run under virtually identical conditions, stained via the same protocol, scanned at the identical resolution, and processed by KEPLER software in an identical manner. Thus the gel format and coordinates of the kidney and testis sample patterns are rendered quite comparable to the well-studied liver patterns. In many cases, proteins common to two or all three of these tissues (*i.e.*, actin, tubulins, α2u-globulin, SMP30, and stress proteins to name a few) can be compared in assessing the toxic effect of the xenobiotic studied. Because the kidney and the testis represent principle and secondary targets of many xenobiotics, protein pattern alterations studied in these tissues, relative to those occurring in the liver, will broaden our understanding of xenobiotic mechanisms.

IPG-DALT. Improving the resolution of basic proteins. Despite its proven utility, the conventional 2D technique used in our studies has inherent difficulty in generating an isoelectric focusing gradient beyond pH 7.0 with broad range BDH 4-8 ampholytes, despite the linearity of the 4-7 pH gradient. Consequently, proteins with alkaline pI (>7.0, such as enoyl CoA hydratase and other notable enzymes) that might be altered by PFDA toxicity are not resolved via the conventional 2D system. One approach to visualizing basic proteins has been to run NEPHGE gels in the first dimension followed by conventional SDS-PAGE in the second (Witzmann *et al.*, 1991a & b). One can visually combine the results of a conventional 2D separation of a protein mixture with its 2D NEPHGE separation, side by side. It would be inherently difficult to image analyze such 2 gel sample separations given the unrealiabilty of both sample application regions on the separate gel patterns. To overcome this problem and thus successfully analyze a wider pH range on single 2D gels, we are currently using "pH Stabilized Gels", a Millipore product which acts as a typical immobilized pH gradient gel (IPG) (*i.e.* Immobiline Dry-Plate IPG, Pharmacia) yet is physically compatible with our ISO-DALT apparatus. The pH Stabilized Gels are 0.75mm tube gels in contrast to the Dry-Plate IPG strips used in horizontal systems (Görg *et al.*, 1986). The exact constituents and their concentrations of the pH Stabilized Gels are proprietary information at this writing. We are testing their suitability in our system and thus have been informed that they are composed of the very same chemicals that are used in the production of conventional IPG strips (4% acrylamide, Fluka Immobilines (pH3-10), urea, NP-40 detergent, and DTT). A representative gel pattern is shown in the videoprint (Fig. 21). We intend to rerun all the samples from the liver study already reported and compare, via image analysis, the improvements and the retrogression of 2D pattern quality.

CONCLUSION

This annual report has summarized the progress made during the research period 1 Apr 93 through 30 Mar 94. With respect to the three objectives originally set forth in the grant proposal, significant progress has been made in the first two, *i.e.* the characterization of perfluorocarboxylic acid toxicity with regard to rodent liver, kidney and testis and comparison of the effects of other related xenobiotics. In this regard it has become evident that, while PFDA, clofibrate, and DEHP have some toxicologic endpoints in common, their effects on the liver's 2D protein pattern are rather diverse. Furthermore, the effects observed in the principal target are manifest in other tissues, such as the kidney and can be studied there as well. Several candidate proteins have been identified as potentially important biomarkers of hepatotoxicity.

We have also taken steps to improve the resolution of basic proteins using pH stabilized first dimension gels, a second and principally technical objective. Later in the research period, IPG strips will be used as first dimension separation, and their use in a so-called IPG-DALT system will be assessed.

Current experiments and those planned for the next research period involve the expansion of the database via protein identification, both in this lab as well as via collaboration; comparison of classical peroxisome proliferators through rigorous dose-response design and a search for threshold-effect pattern alterations; assessment of IPG, pH stabilized and conventional 2D separations; and a preliminary comparison of *in vivo vs. in vitro* 2D Electrophoretic toxicologic analysis. With the latter, the third and final objective of this research project will be addressed.

Publications resulting from this effort:

Witzmann, F.A., B.M. Jarnot, and D.N. Parker. Induction of enoyl-CoA hydratase by LD50 exposure to perfluorocarboxylic acids detected by two-dimensional electrophoresis. Toxicology Letters (in press) 1994.

Witzmann, F.A., B.M. Jarnot, D.N. Parker, and J.W. Clack. Modification of hepatic immunoglobulin heavy chain binding protein (BiP/Grp78) following exposure to structurally diverse peroxisome proliferators. Fundamental and Applied Toxicology (in press) 1994.

Witzmann, F.A. and B.M. Jarnot. Charge modification in rodent hepatic Grp78/BiP following exposure to structurally diverse peroxisome proliferators. Applied and Theoretical Electrophoresis (in press) 1994.

Papers presented at scientific meetings:

Application of 2D electrophoresis and image analysis to perfluorocarboxylic acid toxicology. Large Scale 2-D User's Conference and Workshop, September 8-10, 1993, Center for Advanced Biotechnology Research, Rockville MD.

Witzmann, F.A., J.W. Clack, B.M. Jarnot, and D.N. Parker. Modifications in BiP following exposure to structurally diverse peroxisome proliferators detected by two-dimensional electrophoresis. Presented at the Electrophoresis '93 Meeting, Wild Dunes Resort, Charleston SC, Nov 7-10, 1993

BIBLIOGRAPHY

Andersen, M.E., Baskin, G. and Rogers, A.M. *The Toxicologist* 1:16, 1981.

Anderson, N.L. *Two-dimensional Electrophoresis: Operation of the ISO-DALT System*, Large Scale Biology Press, Washington DC, pp. 3-15, 142, 1988.

Anderson, N.L. In: *New Horizons in Molecular Toxicology* (G.S. Probst, Ed.), pp. 65-71, FASEB, Bethesda MD. 1990.

Anderson, N.L. and Anderson, N.G. *Electrophoresis* 12:883-906, 1991.

Anderson, N.L., Copple, D.C., Bendele, R.A., Probst, G.S., & F.C. Richardson. *Fund. Appl. Toxicol.* 18, 570-580, 1992.

Anderson, N.L., Giere, F.A., Nance, S.L., Gemmell, M.A., Tollaksen, S.L., & N.G. Anderson. *Fund. Appl. Toxicol.* 8, 39-50, 1987.

Anderson, N.L., Esquer-Blasco, R., Hofmann, J.P. and Anderson, N.G. *Electrophoresis* 12:907-930, 1991.

Arnott, D., Shabanowitz, J. and Hunt, D.F. *Clin. Chem.* 39:2005-2010, 1993.

Fujita, T., Uchida, K. and Maruyama, N. *Biochim. Biophys. Acta* 1116:122-128, 1992.

George, M.E. and Andersen, M.E. *Toxicol. Appl. Pharmacol.* 85:169-180, 1986.

Görg, A., Postel, W., Günther, S. and Weser, J., In: Electrophoresis '86, Dunn, M.J. (Ed.), VCH Verlagsgesellschaft, Weinheim, pp. 435-449, 1986.

Hendershot, L.M., Ting, J., and Lee, A.S. *Mol. Cell. Biol.* 8:4250-4256, 1988.

Hochstrasser, D.F., Frutiger, S., Paquet, N. *et al., Electrophoresis* 13:992-1001, 1992.

Hughes, G., Frutiger, S., Paquet, N. *et al., Electrophoresis* 13:707-714, 1992.

Leno, G.H. and Ledford, B.E. *FEBS Lett.* 276:29-33, 1990.

Leustek, T., Amir-Shapira, D., Toledo, H., Brot, N., and Weissbach, H. *Cell. Mol. Biol.* 38:1-10, 1992.

Lock, E.A. In: *Renal Disposition and Nephrotoxicity of Xenobiotics*, Anders, M.W. (Ed.), Academic Press, New York, pp.217-233, 1993.

Martin, J.L., Kenna, J.G., Martin, B.M., and Pohl, L.R. *Toxicologist* 9:5, 1989.

Neidhardt, F.C., Appleby, D.A., Sankar, P. Hutton, P, and Phillips, T.A. *Electrophoresis* 10:116-121, 1989.

Neuhoff, V., Arold, N., Taube, D., and Ehrhardt, W. *Electrophoresis* 9:255-262, 1988.

Okita, J.R, Castle, P.J., and Okita, R.T. *J. Biochem. Toxicol.* 8:135-144, 1993.

Olson, C.T. and Andersen, M.E. *Toxicol. Appl. Pharmacol.* 70:362-372, 1983.

Pappin, D.J.C., Hojrup, P., and Bleasby, A.J. *Current Biology* 3:327-332, 1993.

Richardson, F.C., Strom, S.C., Copple, .M., Bendele, R.A., Probst, G.S., & Anderson, N.L. *Electrophoresis* 14:157-161, 1993.

Tata, J.R. In: *Subcellular Components* (G.D. Birnie, Ed.), pp. 185-214. Butterworths, London.1972.

Vanden Heuvel, J.P., Kuslikis, B.I., Van Rafelghem, M.J., and R.E. Peterson. D. *Toxicol. Appl. Pharmacol.* 107:450-459, 1991a.

Vanden Heuvel, J.P., Kuslikis, B.I., Van Rafelghem, M.J., and R.E. Peterson. *J. Biochem. Toxicol.* 6:83-92, 1991b

Witzmann, F.A. and Parker, D.N. *Toxicol. Letters* 57:29-36, 1991a.

Witzmann, F., Jarnot, B., and Parker, D. *Electrophoresis* 12:687-688, 1991b.

Witzmann, F.A., Jarnot, B.M., and Clack, J.W. *Appl. Theoret. Electrophoresis*. in press, 1994a.

Witzmann, F.A., Jarnot, B.M., Parker, D.N., and Clack, J.W. *Fund. Appl. Toxicol.* in press, 1994b.

ADDENDUM A

FIGURE 1

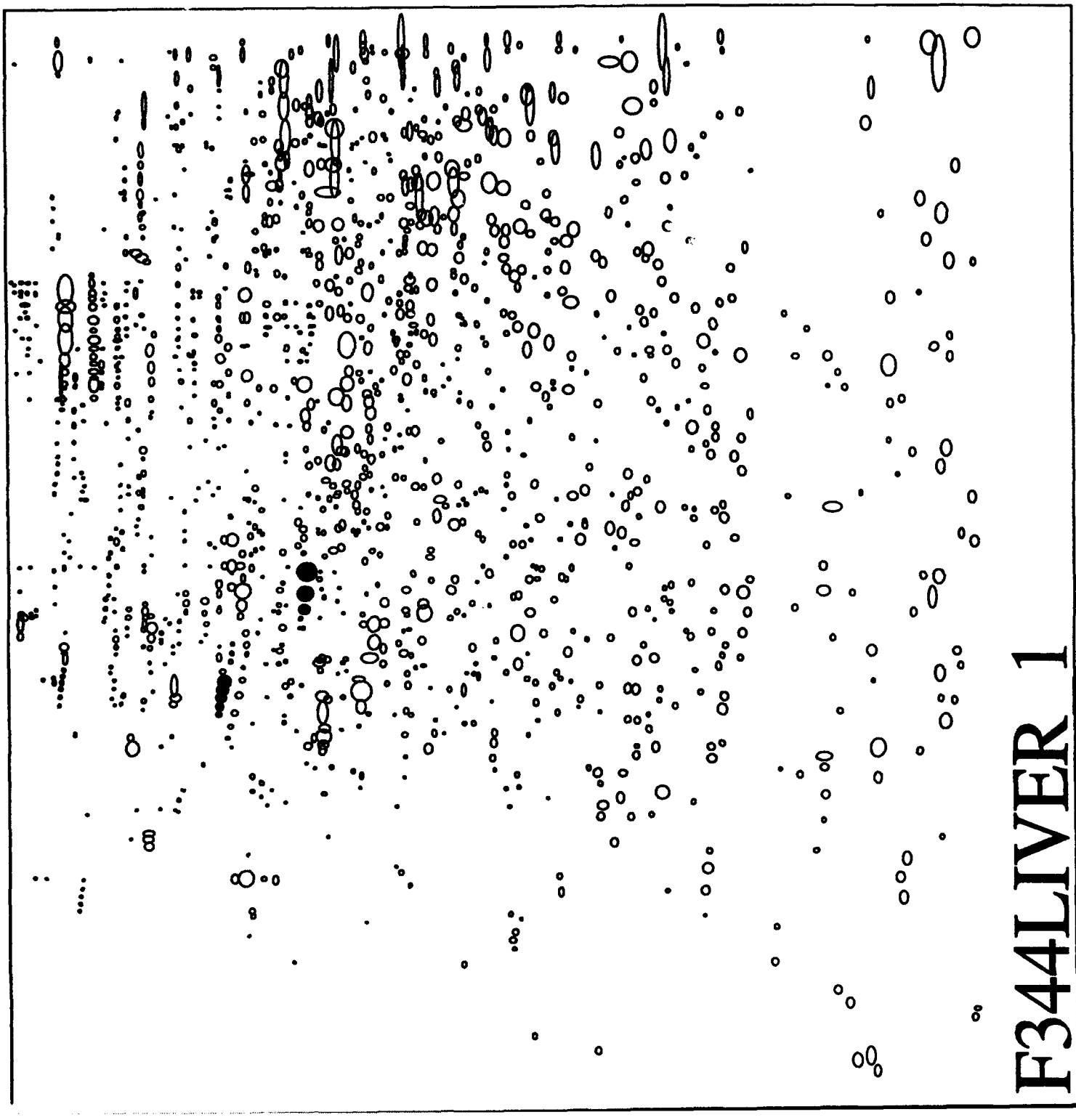
F34LIVER 1
Grp78/BiP and Hsp60 Rat Liver Whole Homogenate
Experiment LTK_LIVER
11:02 21-OCT-93

FIGURE 2A

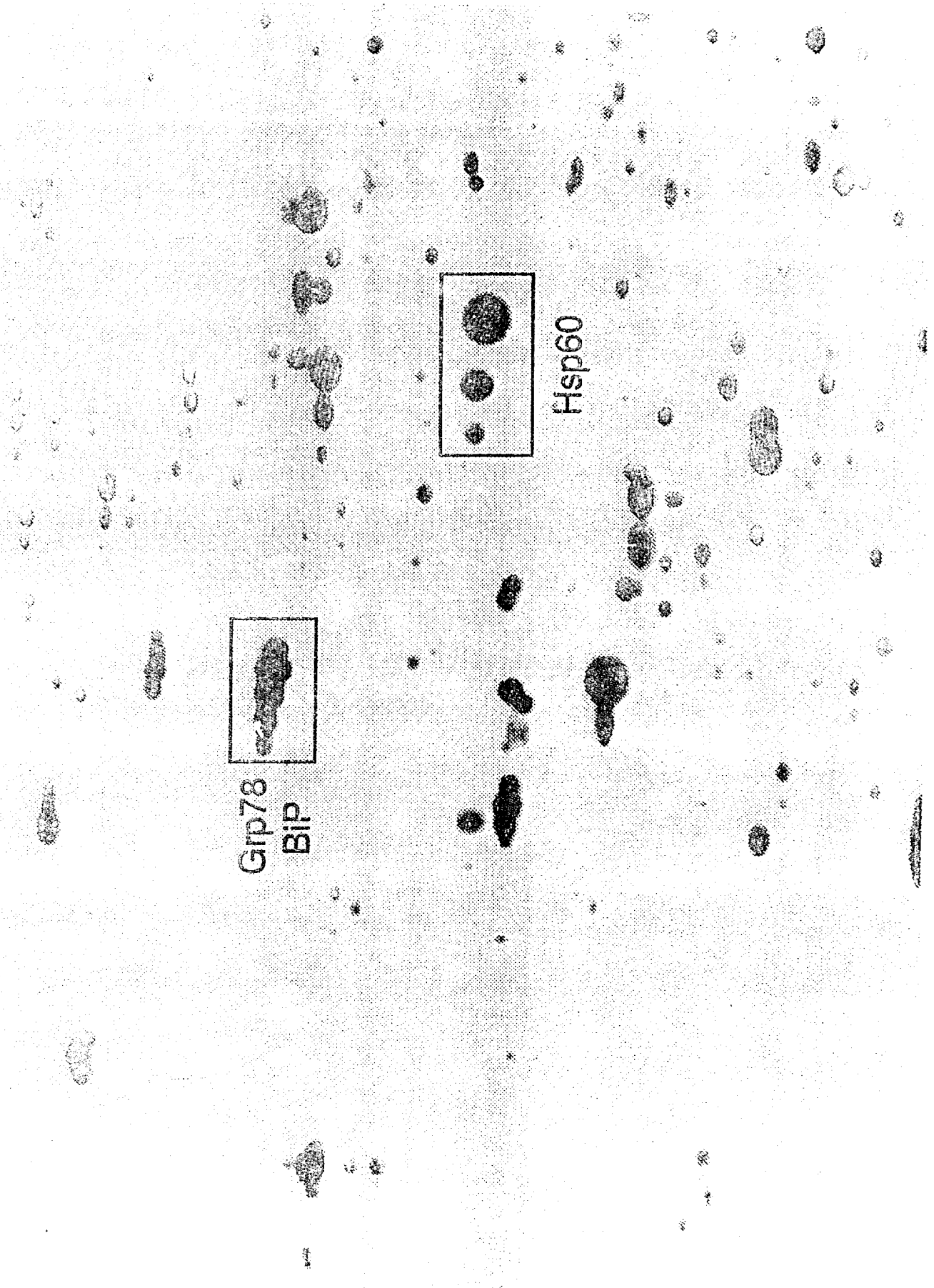

FIGURE 2B

FIGURE 3

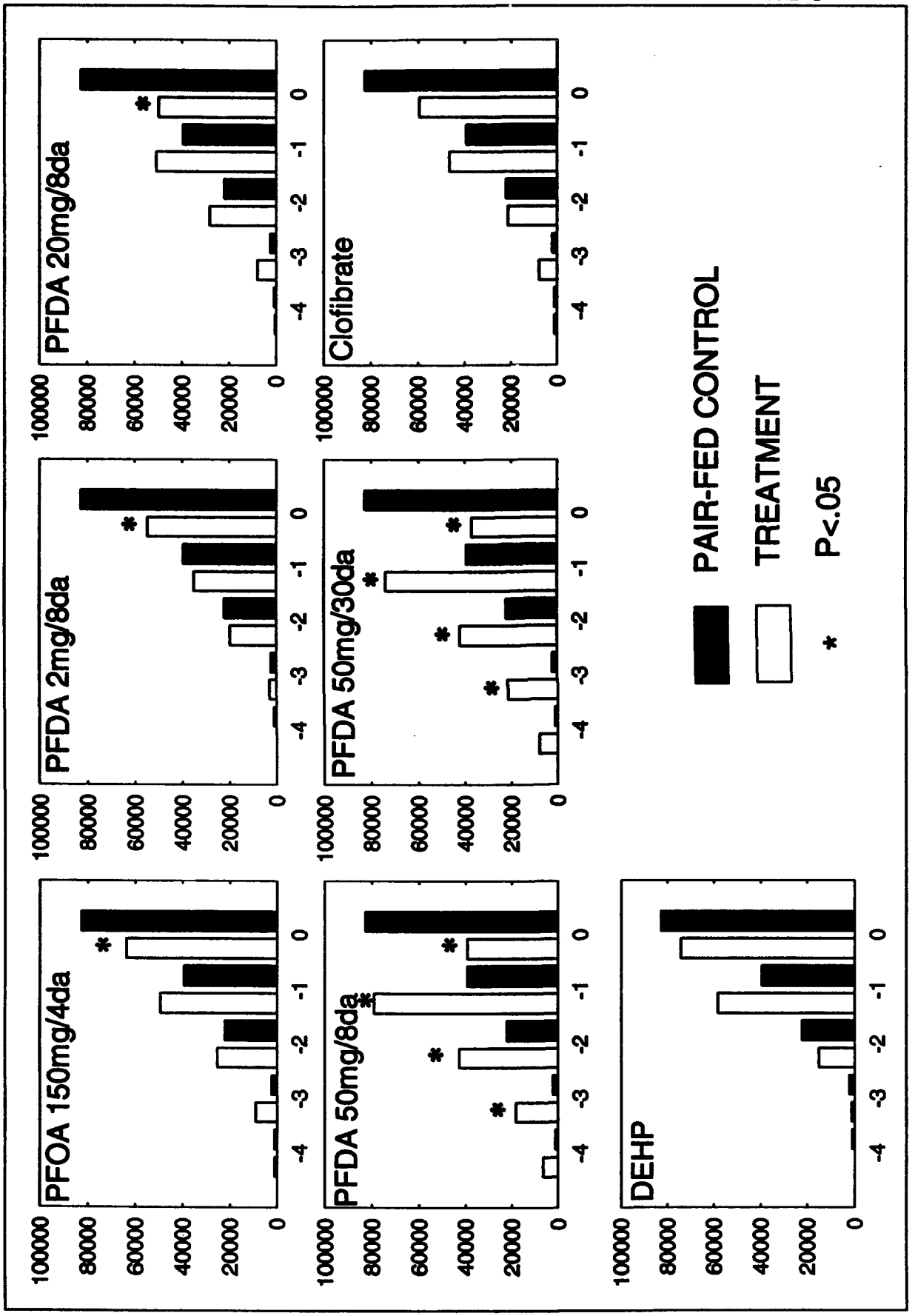
Abundance
PFOA 150mg/4da
PFDA 2mg/8da
PFDA 20mg/8da
PFDA 50mg/8da
PFDA 50mg/30da
Clofibrate
DEHP
100000
80000
60000
40000
20000
0
-4
-3
-2
-1
0
PAIR-FED CONTROL
TREATMENT
P<.05
Molecular Charge Relative to Major Form

FIGURE 4

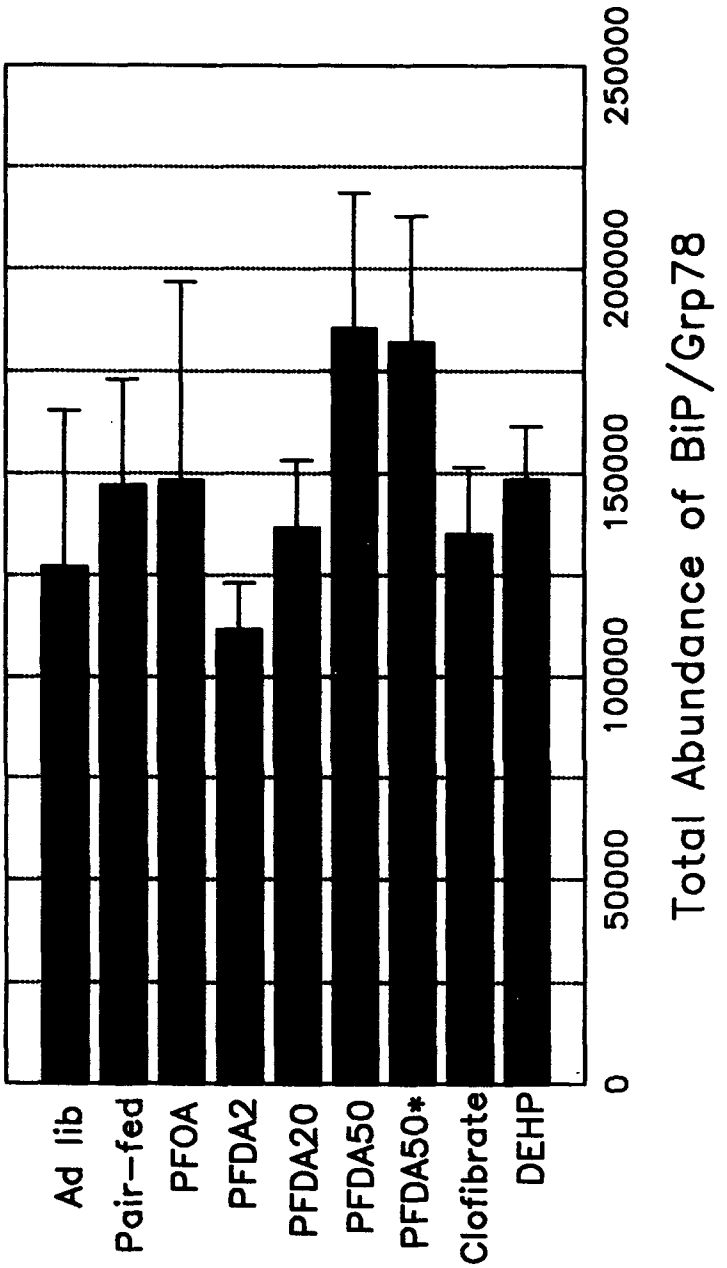
Total Abundance of BiP/Grp78
0
50000
100000
150000
200000
250000
Ad lib
Pair-fed
PFOA
PFDA2
PFDA20
PFDA50
PFDA50*
Clofibrate
DEHP

FIGURE 5

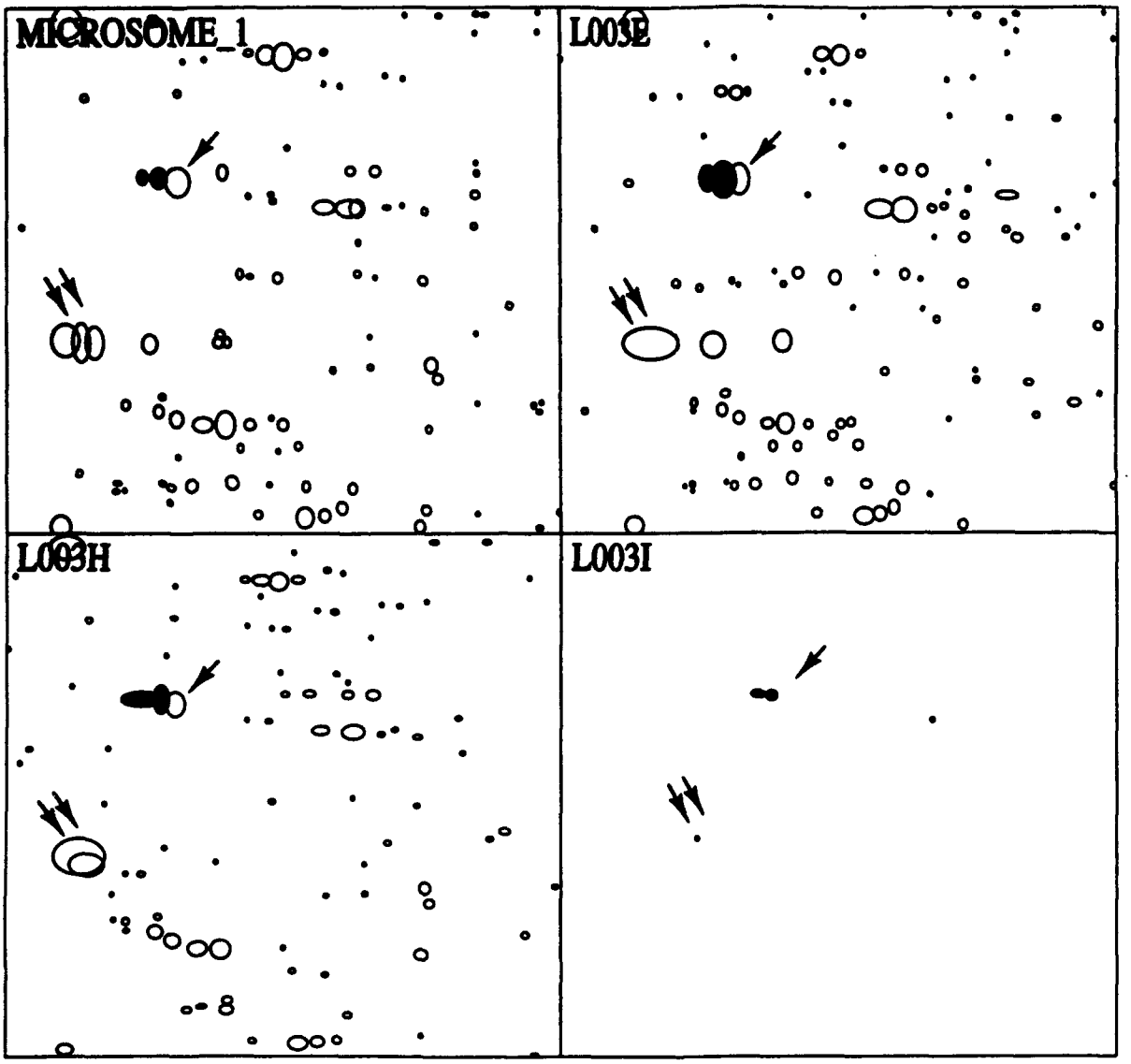

FIGURE 6

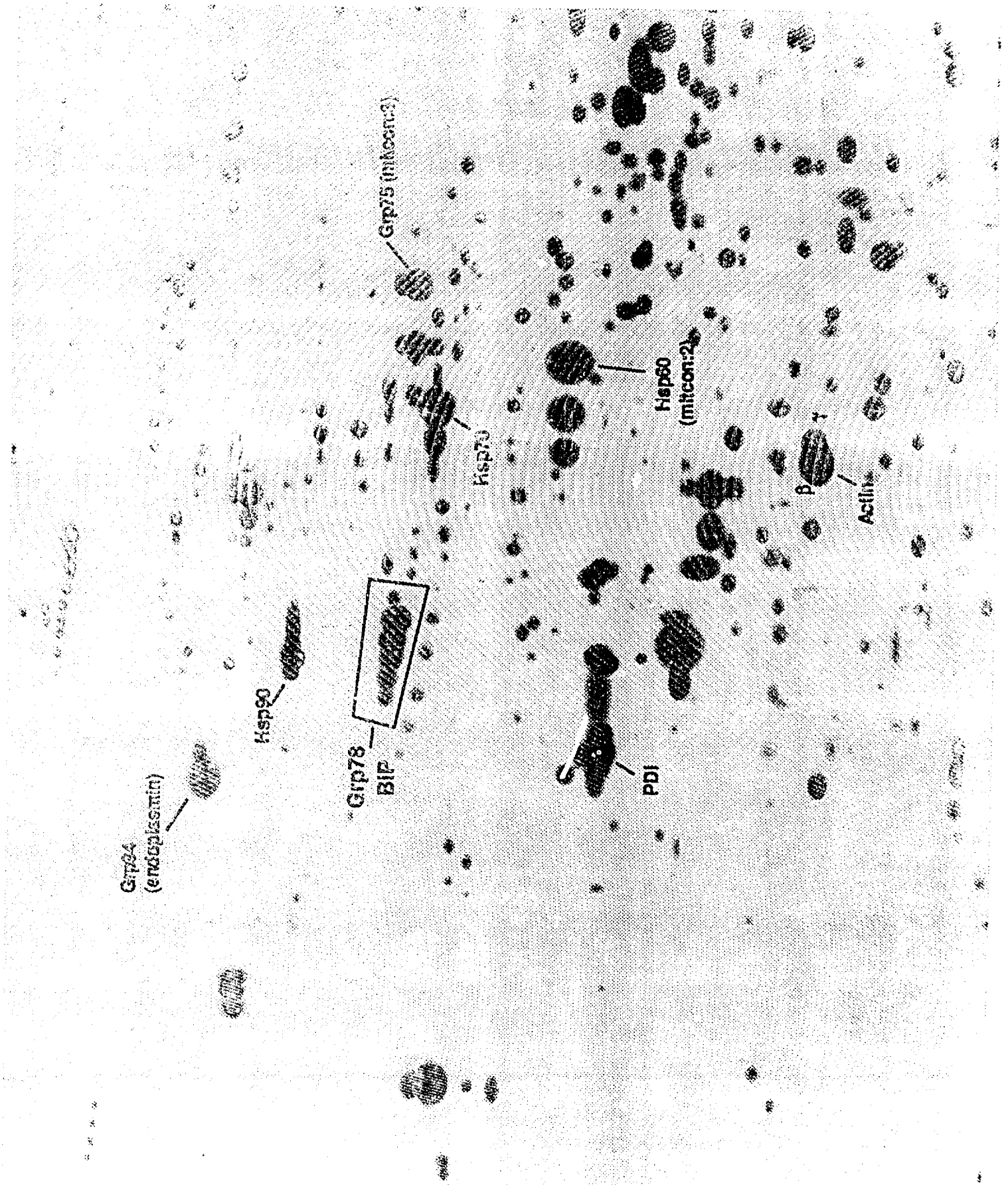
Grp94
(endoplasmin)
Hsp90
Grp78
BIP
Grp75 (mitcon:3)
Hsp70
Hsp60
(mitcon:2)
PDI
β
Actin

FIGURE 7

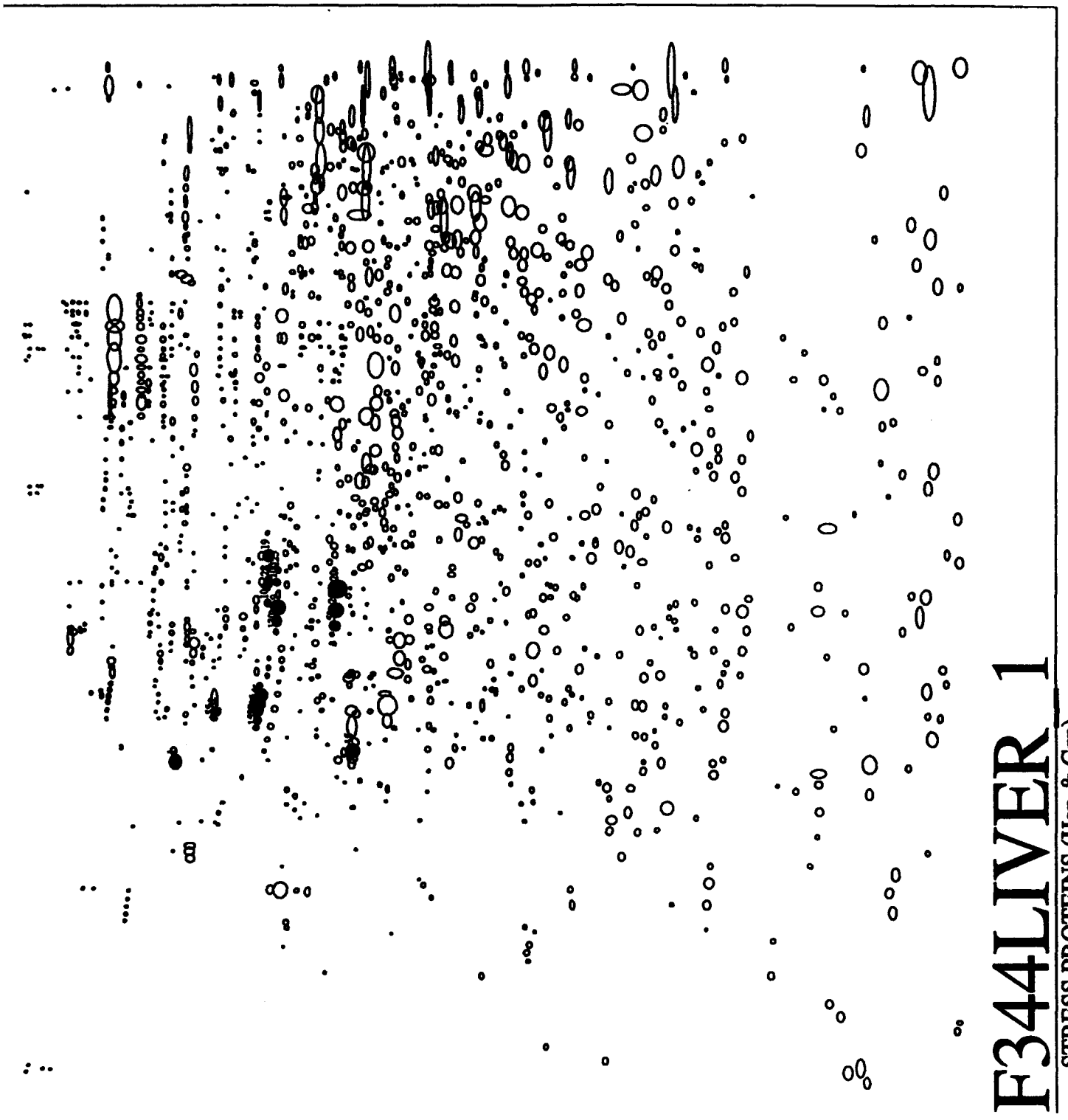
F34LIVER 1
STRESS PROTEINS (Hsp & Grp)
Experiment LTK_LIVER
13:50 18-APR-94

Figure 8. Illustrated below are the stress proteins and their charge variants and the effect of various exposures on their abundance. In each numbered frame, the number is the MSN of theat protein and the bar graphs represent that protein's abundance in each individual sample. From left to right in each frame, the groups are separated by a vertical line as follows, *Ad Lib*; Pair-fed; PFOA 150mg/kg;; PFDA 2mg/kg; PFDA 20mg/kg; PFDA 50mg/kg,8da; PFDA 50mg/kg ,30da; Clofibrate; and DEHP. The triangles appearing beneath some groups indicates a significant difference (P<.001) relative to the *Ad Lib* group via Student's t-Test. Proteins are identified as follows: MSN 1 = GRP94/Endoplasmin; MSN 32 & 55 = Hsp90; MSN 19, 28, and 106 = Grp75; MSN 100 & 123 = HSP70; MSN 9, 24 & 130 = Hsc70.

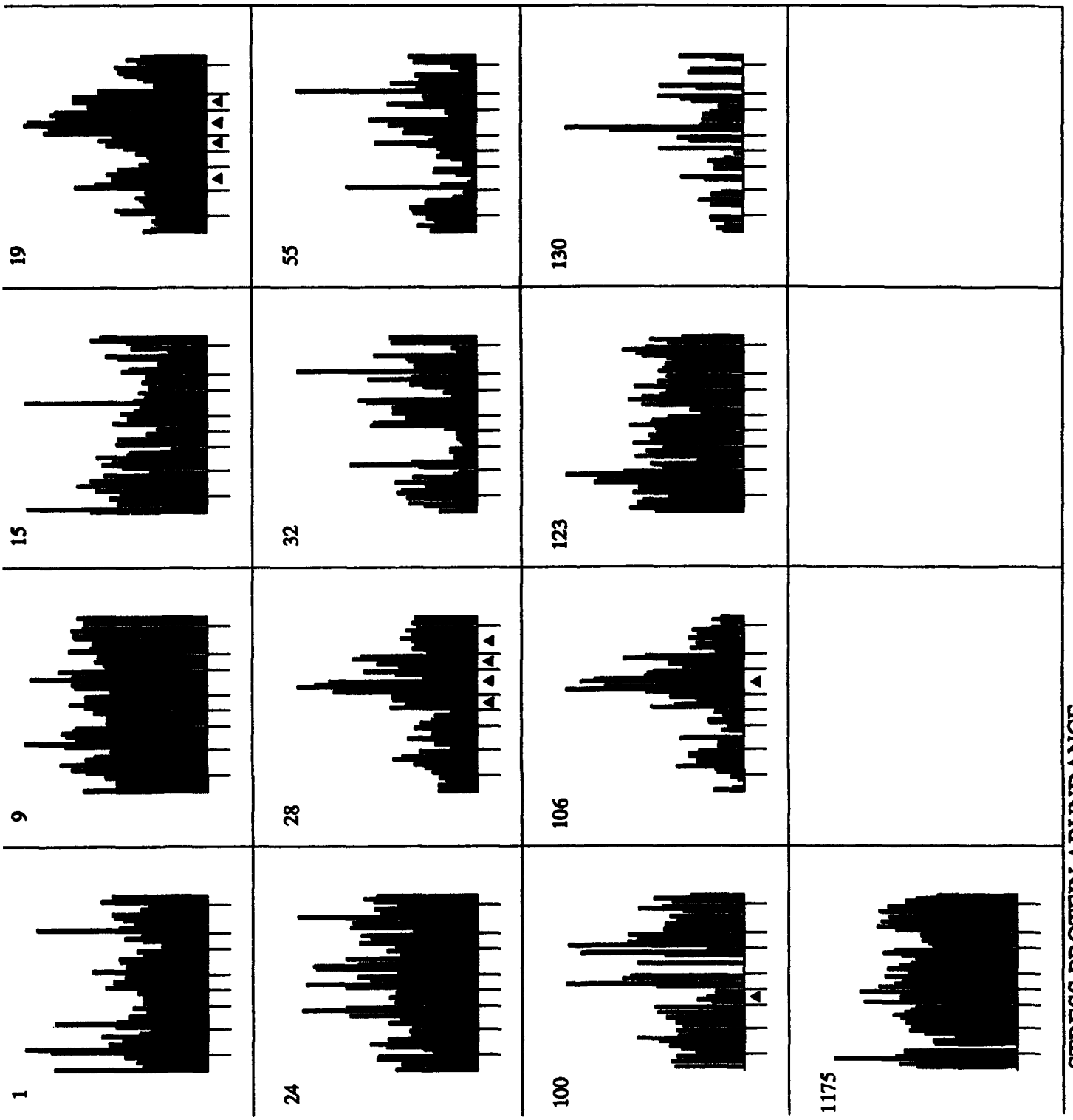

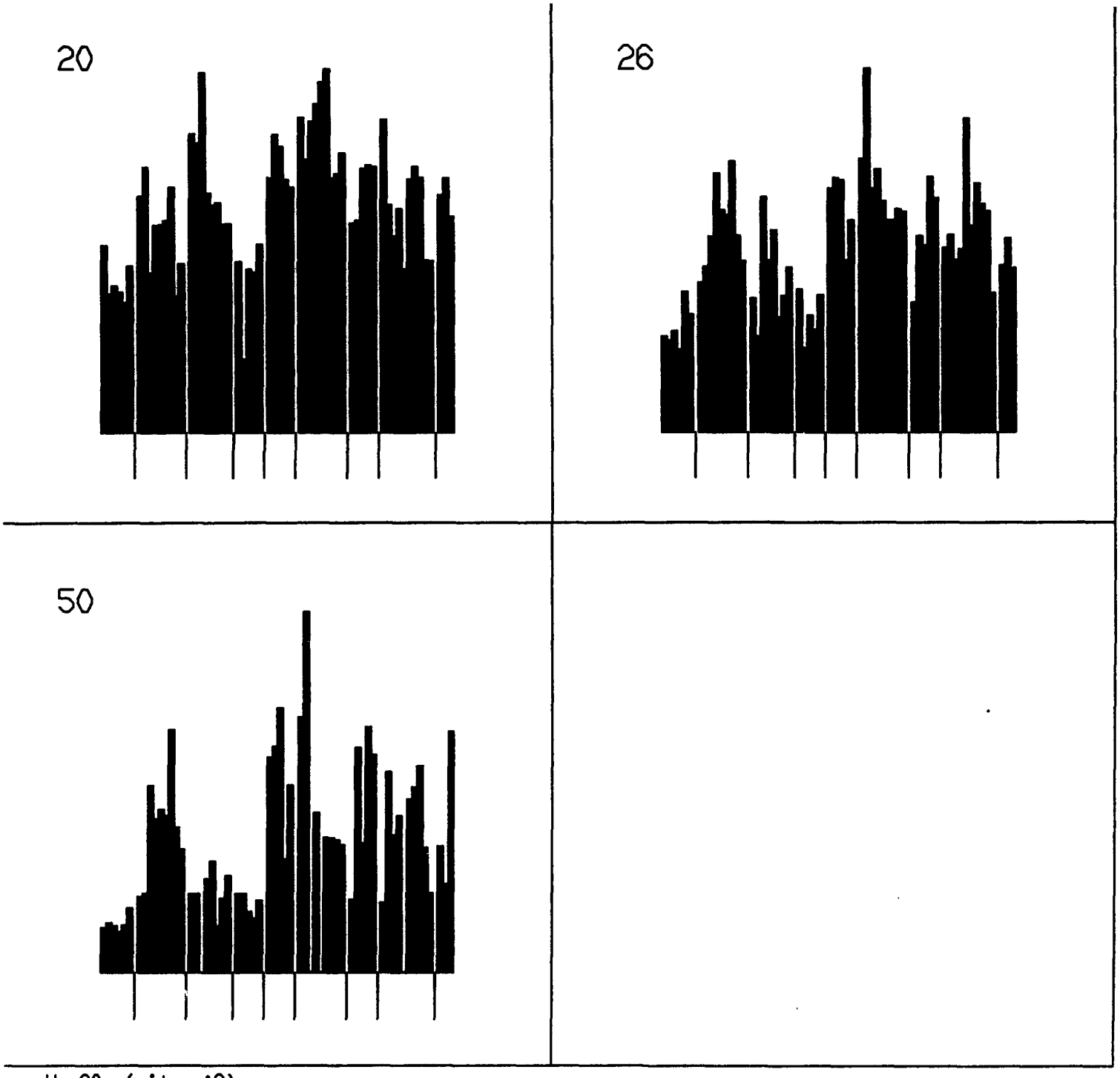

Hsp60 (mitcon:2)
Experiment LTK_LIVER

16:55 29-SEP-93

FIGURE 9A

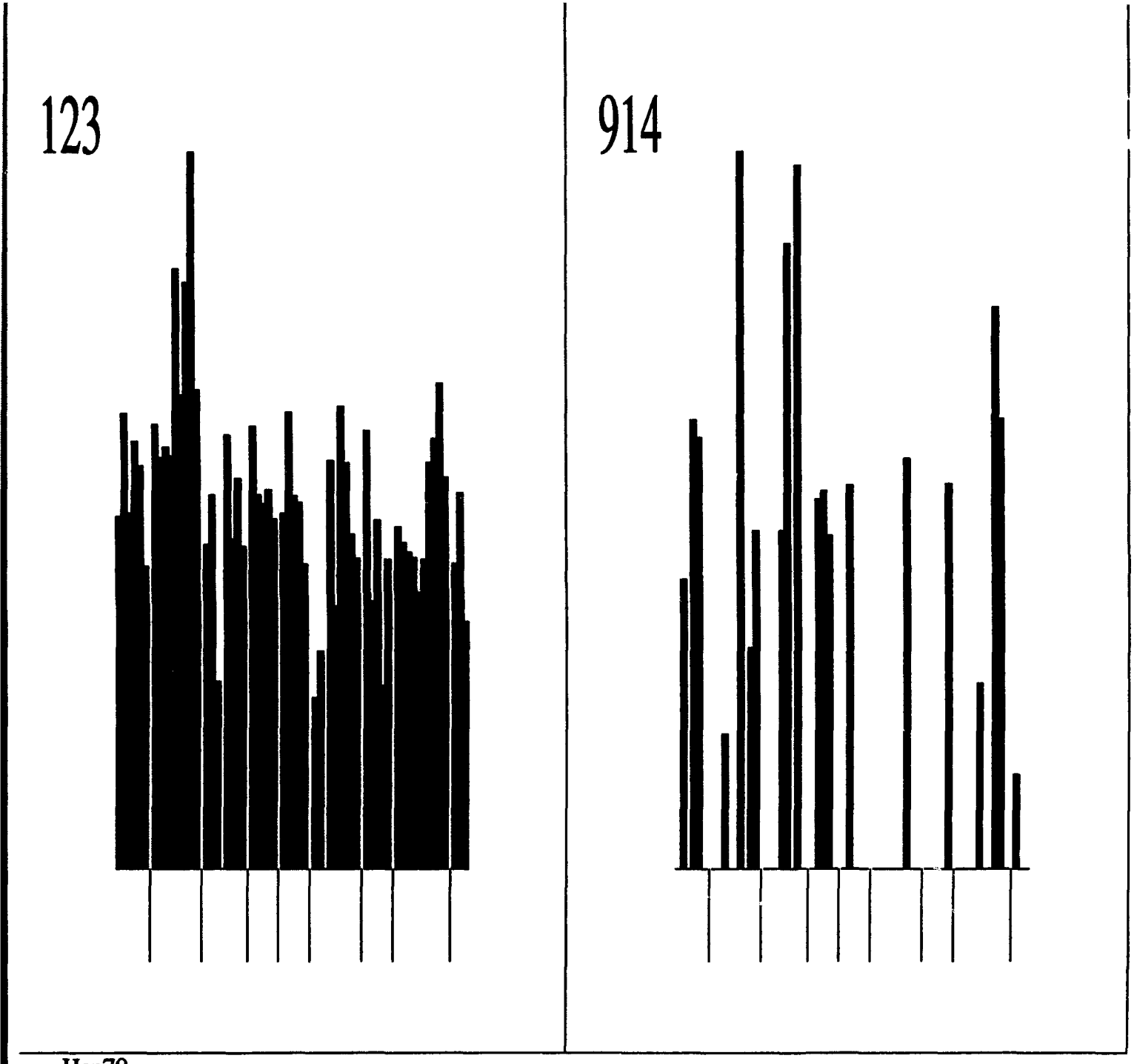

Hsp70
Experiment LTK_LIVER

12:30 4-FEB-94

FIGURE 9B

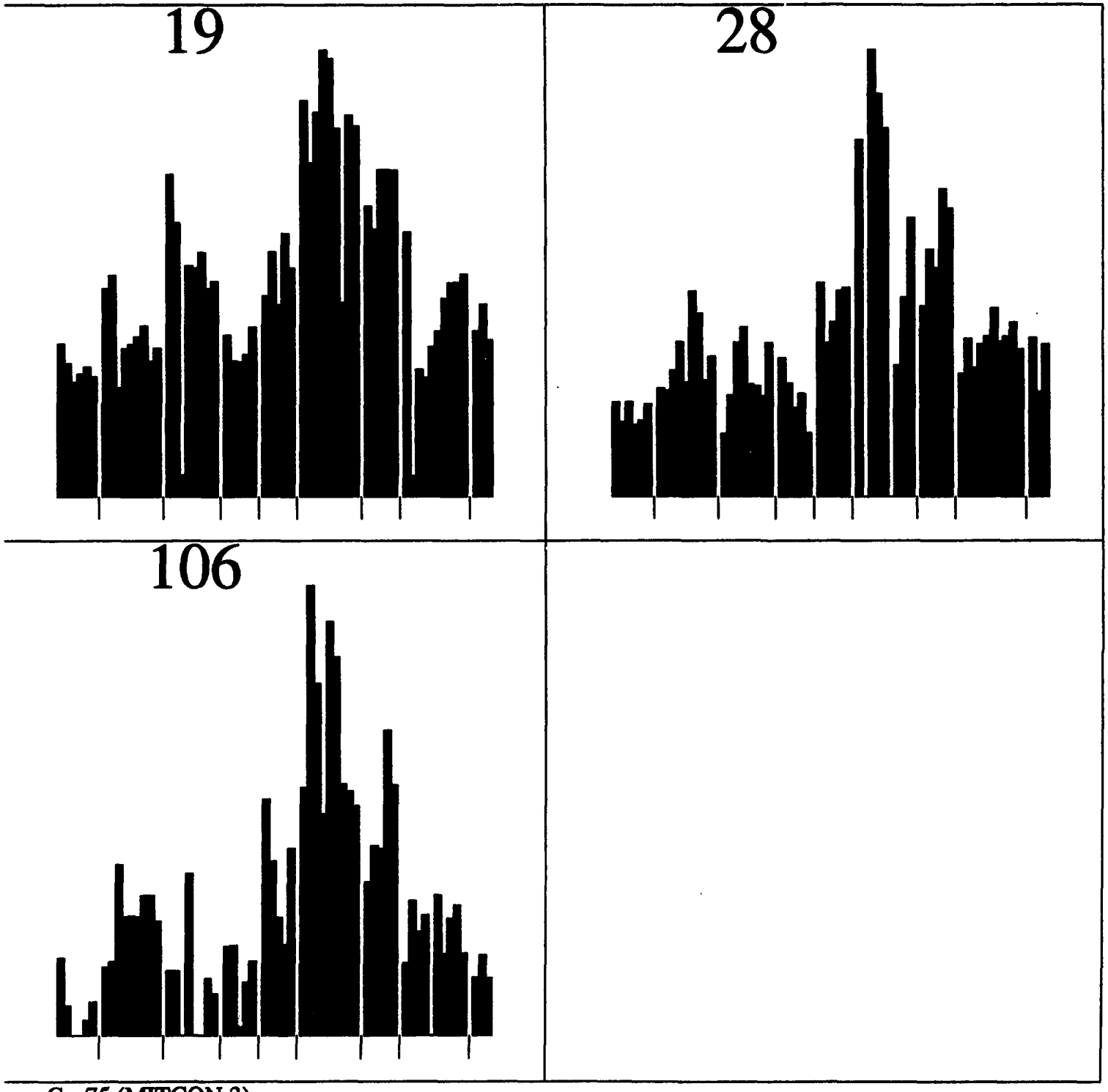

Grp75 (MITCON:3)
Experiment LTK_LIVER

10:20 16-AUG-93

FIGURE 9C

FIGURE 9D

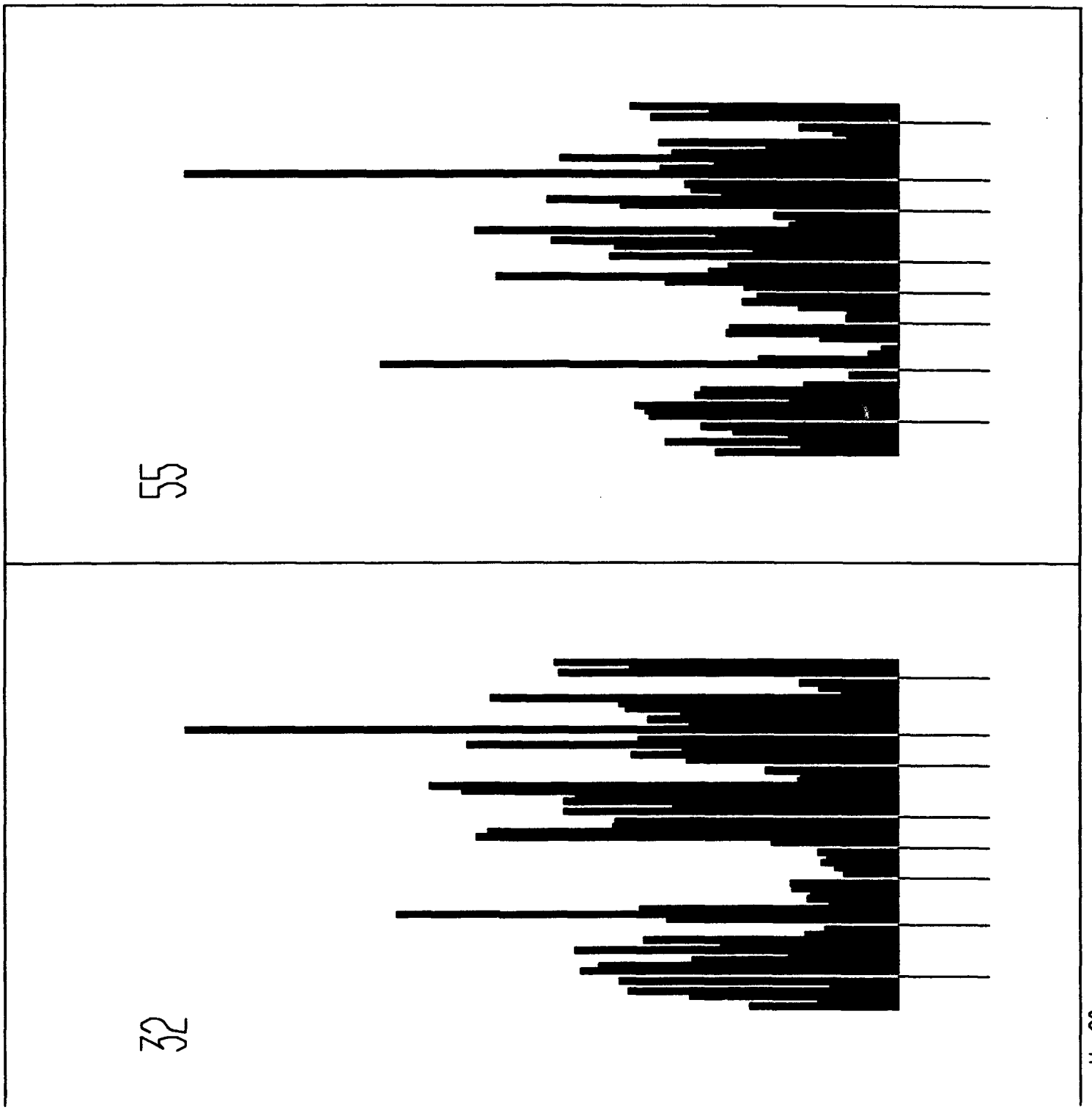

FIGURE 9E

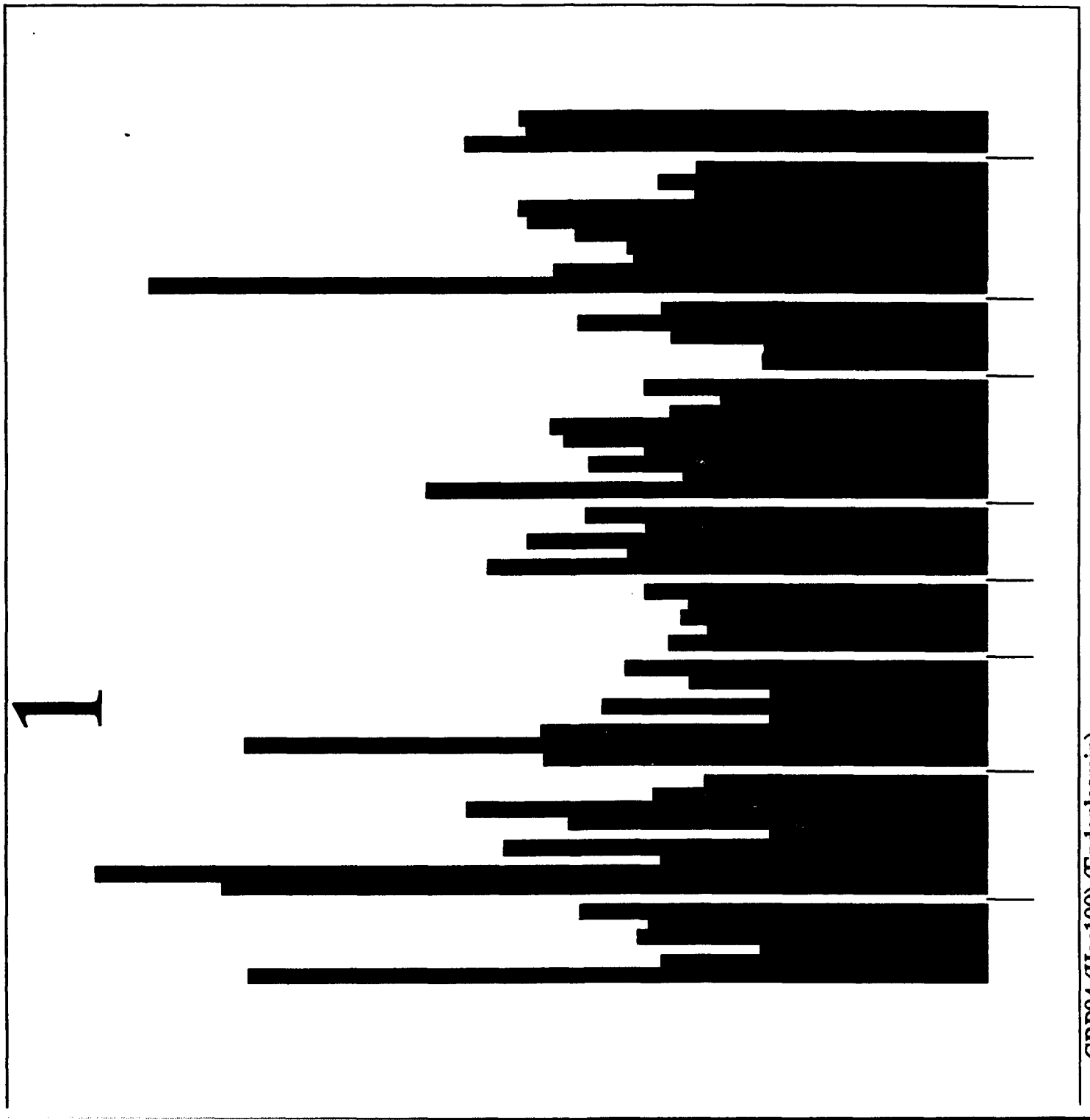
GRP94 (Hsp100) (Endoplasmin)
Experiment LTK_LIVER 12:49 22-JUN-93

FIGURE 10

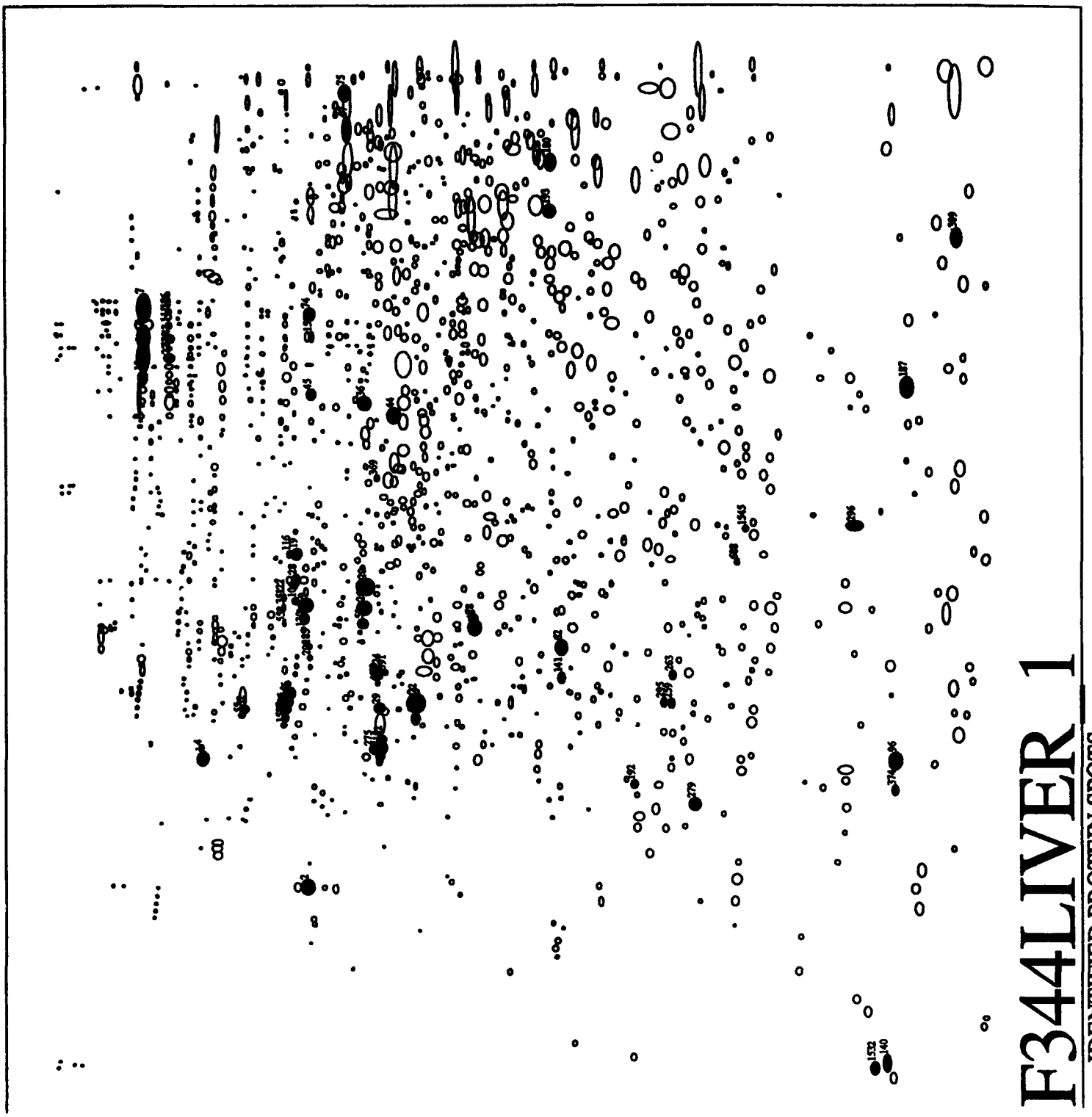
F34LIVER_1
IDENTIFIED PROTEIN SPOTS
Experiment LTK_LIVER
12:34 18-APR-94

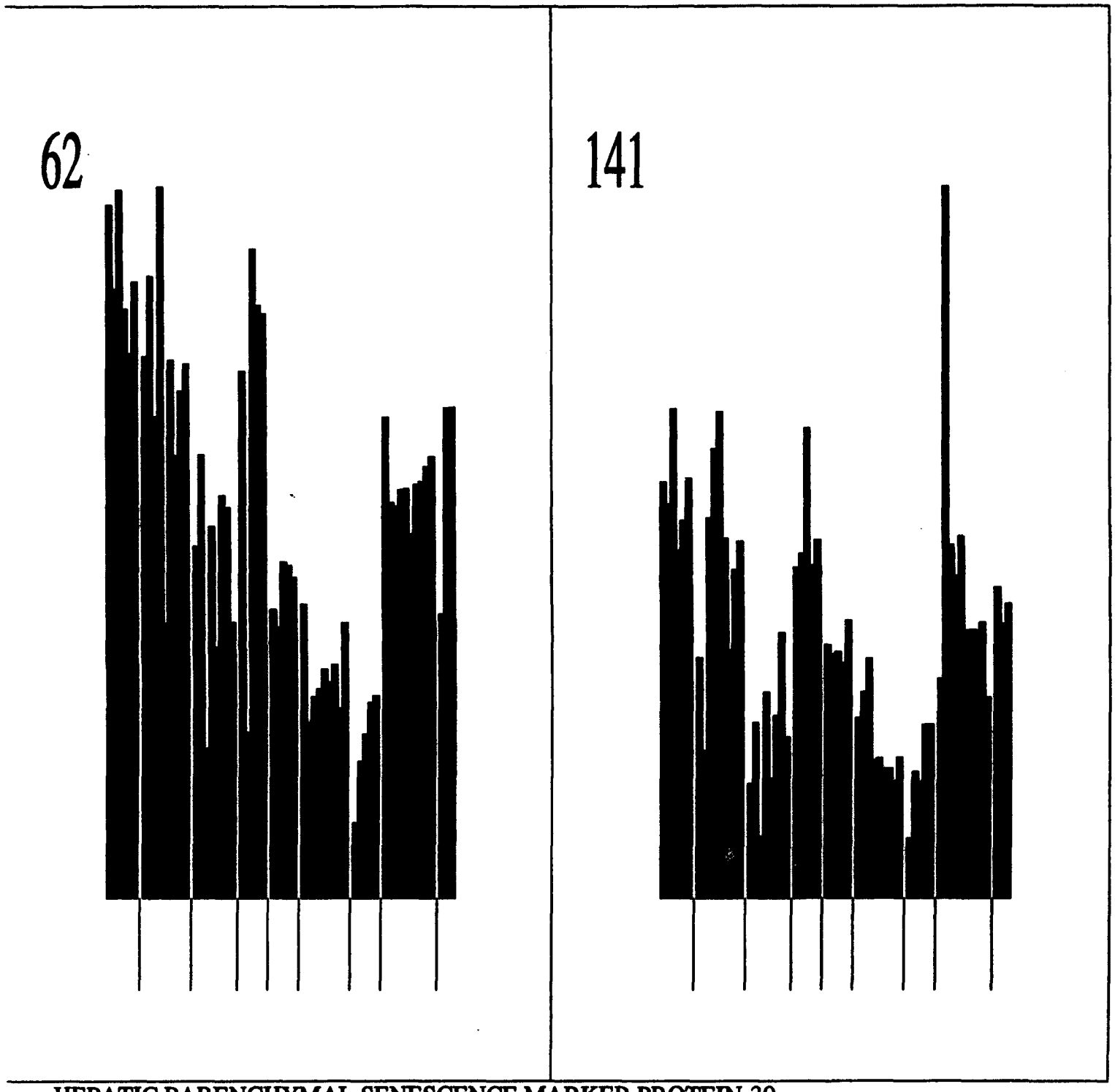

HEPATIC PARENCHYMAL SENESCENCE MARKER PROTEIN-30
Experiment LTK_LIVER 11:55 20-APR-94

FIGURE 11

FIGURE 12

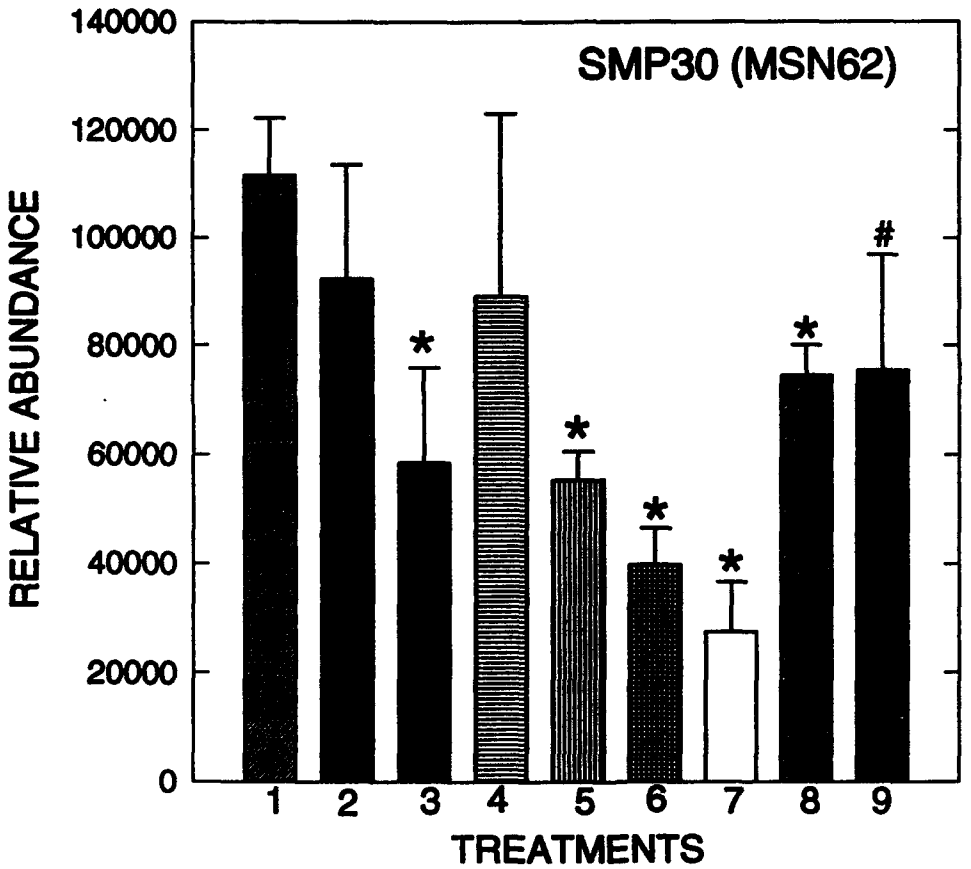
SMP30 (MSN62)
RELATIVE ABUNDANCE
140000
120000
100000
80000
60000
40000
20000
0
1
2
3
4
5
6
7
8
9
TREATMENTS
*
*
*
*
*
#

FIGURE 13

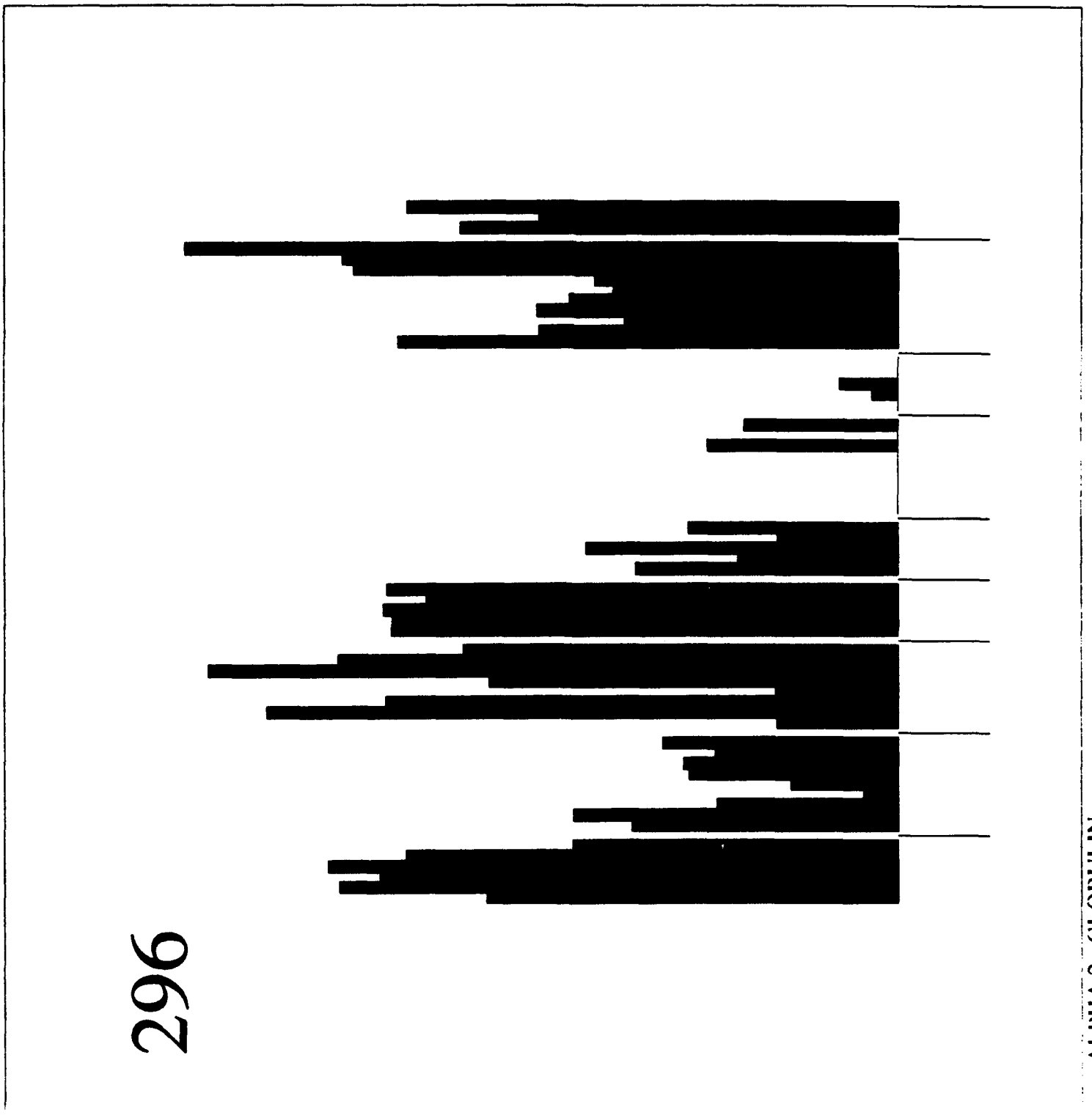

FIGURE 1A

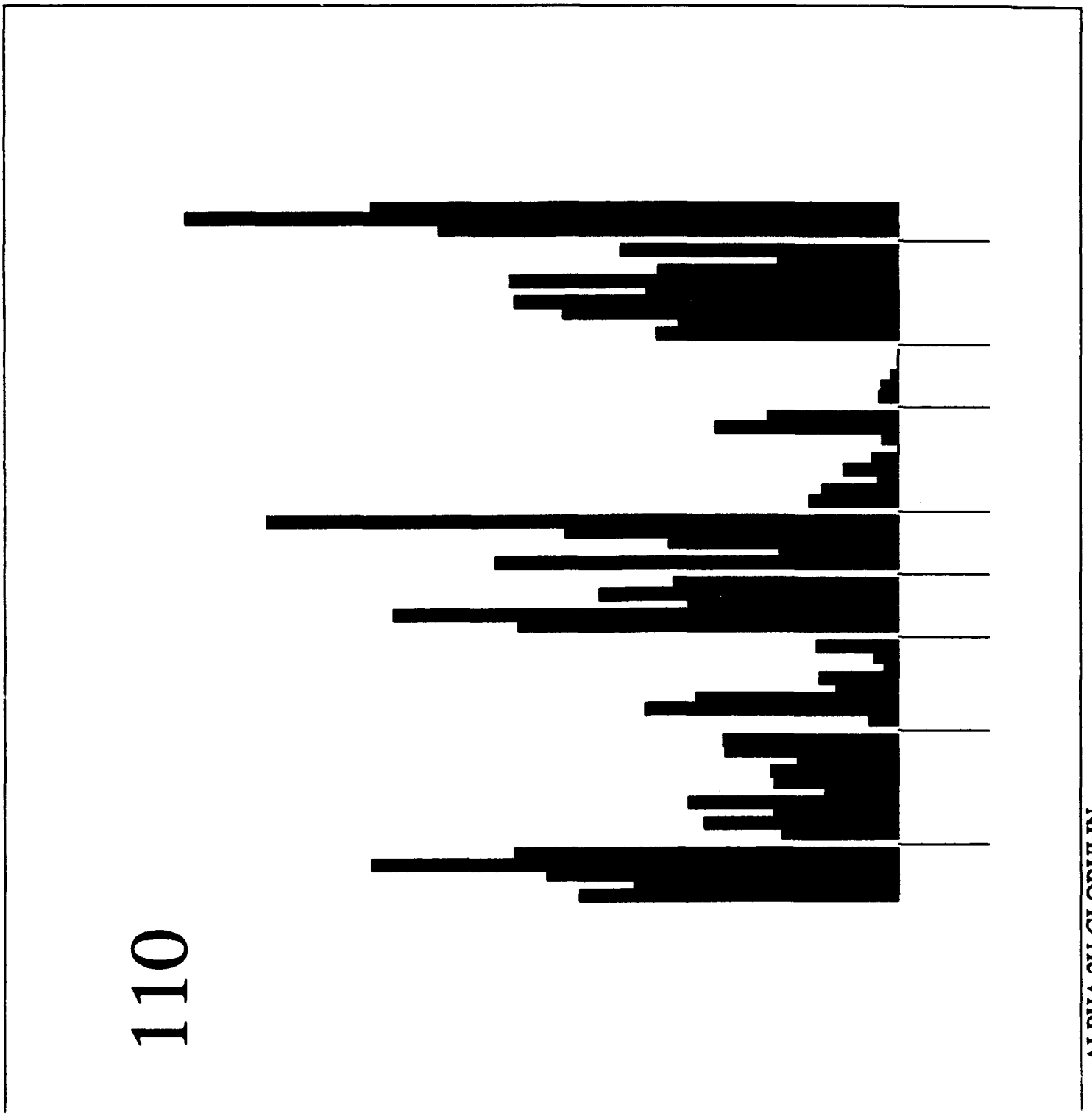

FIGURE 15

Spectrum printed at 16:40 Wed Sep 22 1993

Sample: **4hr digest - speedvac**
Sample No: 0
Comment:

Operator: FAW
Account No:
Data File: C:\LASERMAT\DATA\HBDIGEST.503
Saved on: 16:19 Wed Sep 22 1993

Peak Detection File: C:\LASERMAT\DETECT\DEFAULT.CAL
Calibration: External A: -0.049 B/V: 0.629925
Mass 1: 0.000 Mass 2: 1348.600
No of shots: 20 **Laser Aim: 3** **Laser Power: 33**
Polarity: Positive Accelerating Voltage: 20004 Gain: 31mV

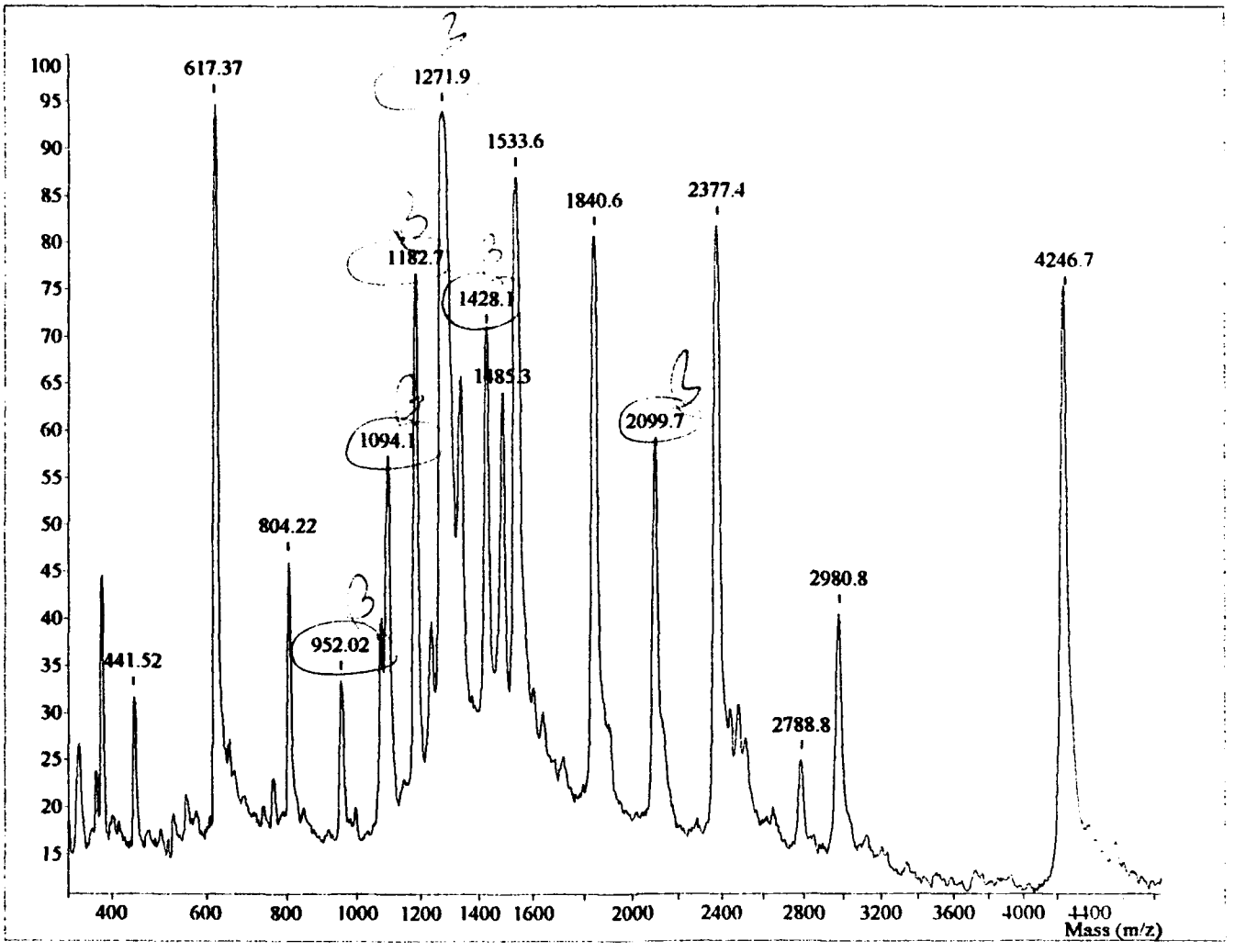

FIGURE 16

Spectrum printed at 18:19 Tue Nov 30 1993

Sample: 3-1
Sample No: 0
Comment:

Operator: Witzmann
Account No:
Data File: C:\LASERMAT\DATA\NOV30.002
Saved on: 17:51 Tue Nov 30 1993

Peak Detection File: C:\LASERMAT\DETECT\APO.CAL
Calibration: External A: -0.049 B/V: 0.629925
Mass 1: 0.000 Mass 2: 1348.600
No of shots: 10 **Laser Aim: 1** **Laser Power: 40**
Polarity: Positive Accelerating Voltage: 20017 Gain: 31mV

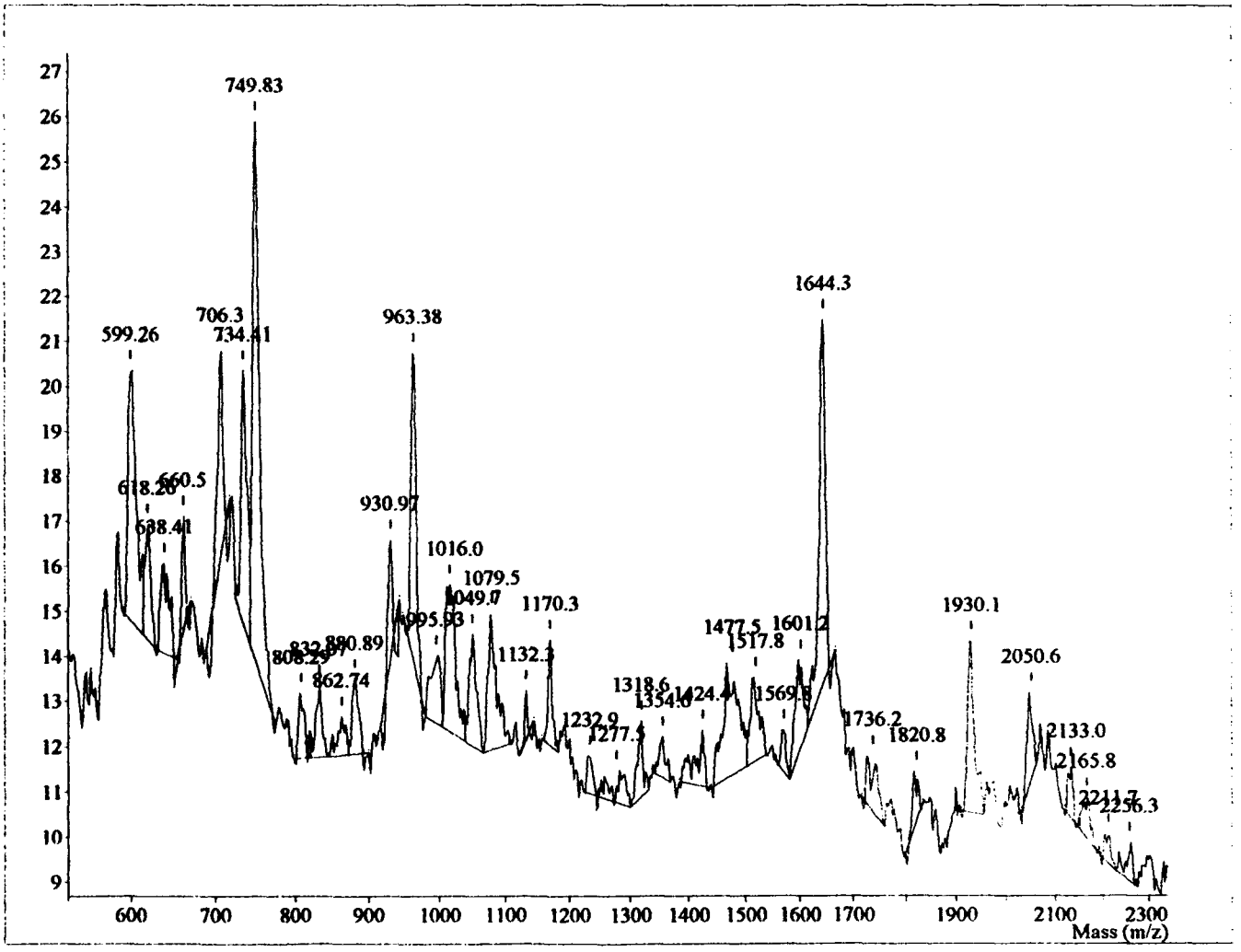

FIGURE 17

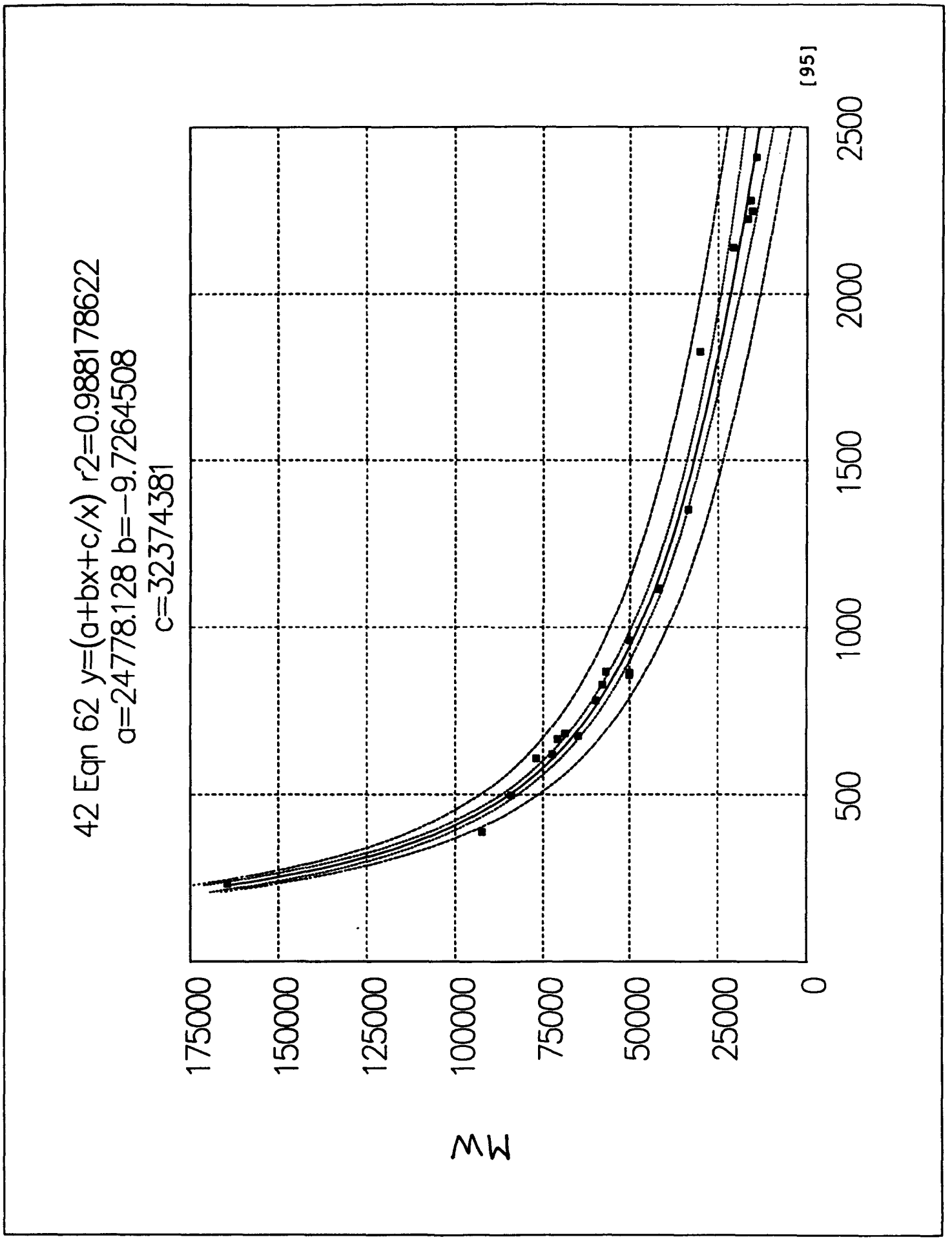
42 Eqn 62 y=(a+bx+c/x) r2=0.98817 8622
a=24778.128 b=-9.7264508
c=32374381
[95]
MW
175000
150000
125000
100000
75000
50000
25000
0
500
1000
1500
2000
2500

FIGURE 18

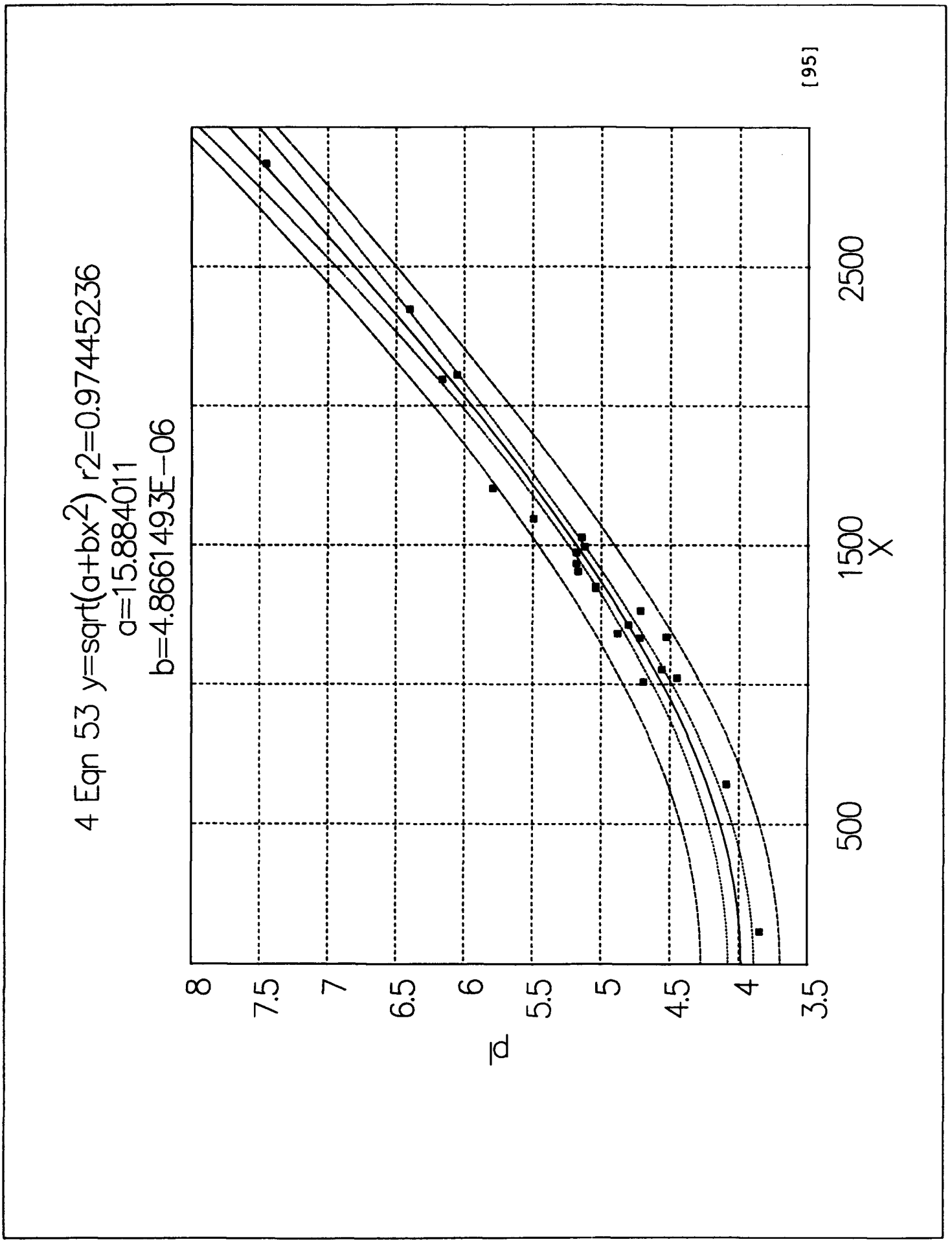
4 Eqn 53 y=sqrt(a+bx^2) r2=0.97445236
a=15.884011
b=4.8661493E-06
[95]
8
7.5
7
6.5
6
5.5
5
4.5
4
3.5
d
500
1500
2500
X

FIGURE 19

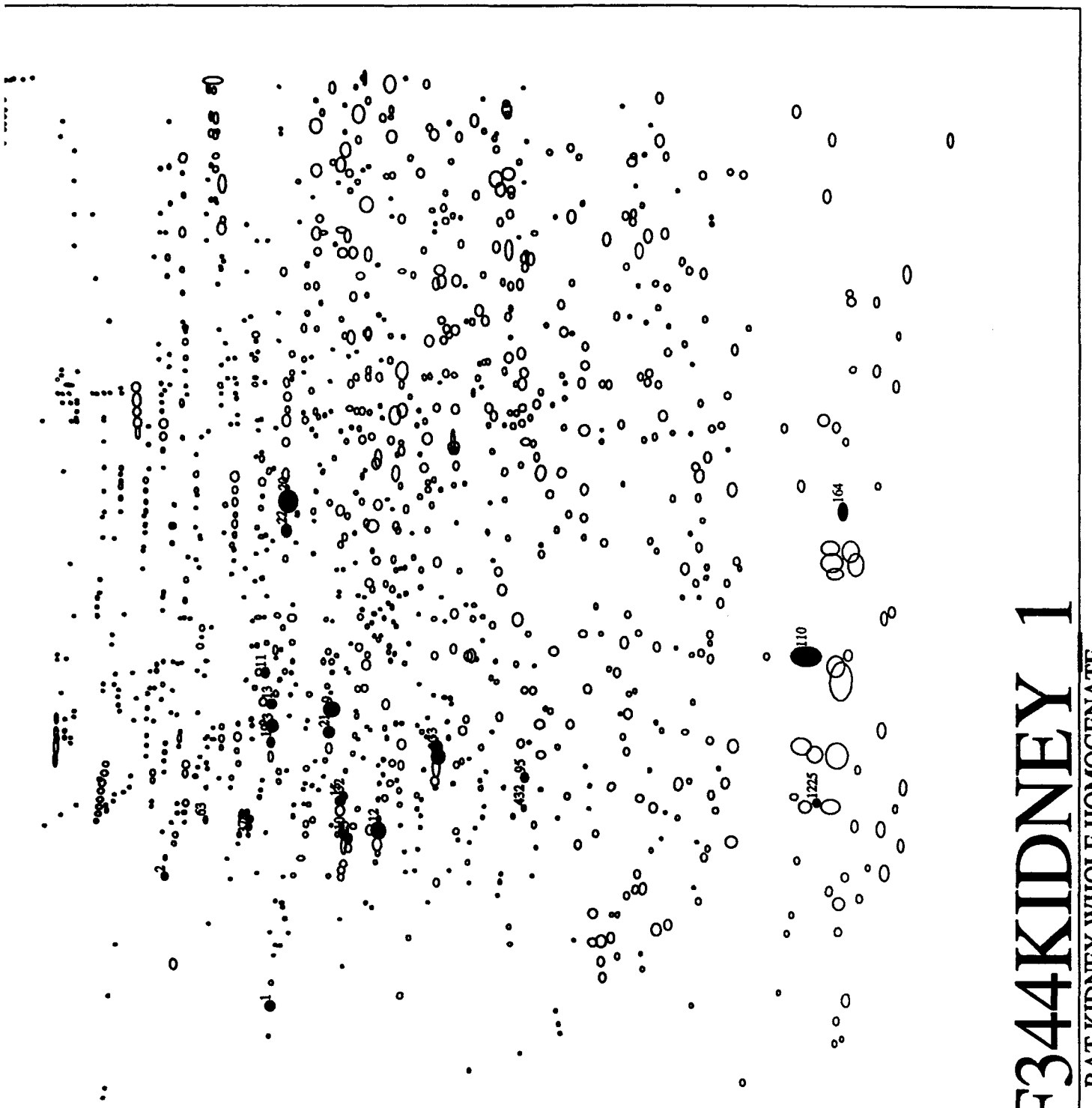
F34KIDNEY 1
RAT KIDNEY WHOLE HOMOGENATE
Experiment LTK_KIDNEY
10:53 21-APR-94

FIGURE 20

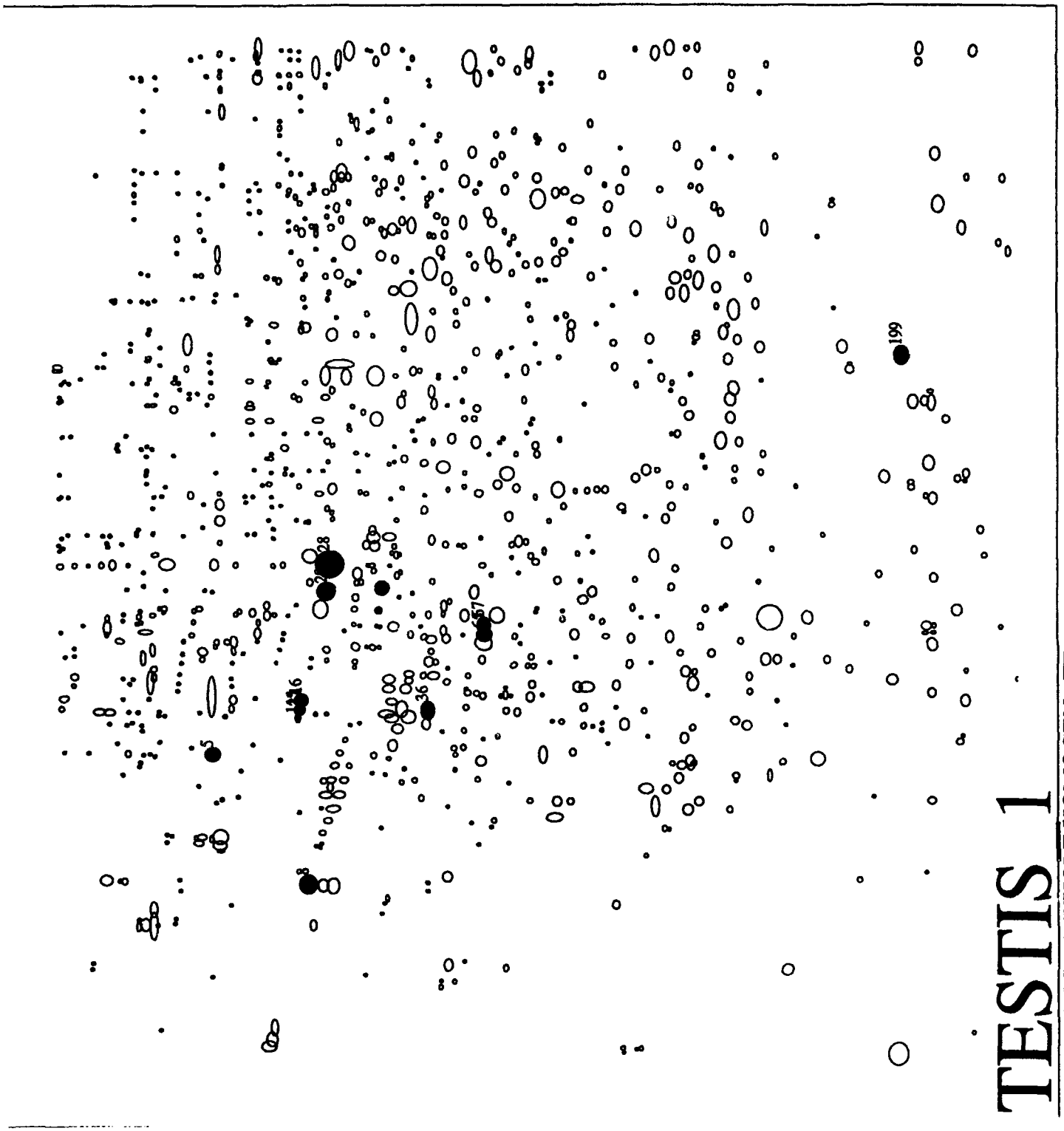
TESTIS 1
RAT TESTIS WHOLE HOMOGENATE
Experiment TESTIS_TOX
11:19 21-APR-94
199
28
36
5

TABLE 3.

F344LIVER_1 Master Pattern Database (Identified Proteins)

MSN	Identification (name)	MW calc.	Y coord.	pI calc.	X coord.	Volume (ave. control)	Reference
180	3-alpha-hydroxysteroid-dihydrodiol dehydrog.	36272	1326.9	7.30	2772.8	52499	immunologic (Anderson et al., Electrophoresis, 1991)
193	3-alpha-hydroxysteroid-dihydrodiol dehydrog.	36371	1323.3	7.04	2830.0	34376	immunologic (Anderson et al., Electrophoresis, 1991)
259	3-hydroxy-3-methylgutaryl CoA synthase	28388	1648.3	4.76	1179.7	7691	immunologic (Anderson et al., Electrophoresis, 1991)
558	3-hydroxy-3-methylgutaryl CoA synthase	72210	607.0	5.07	1418.3	1042	immunologic (Anderson et al., Electrophoresis, 1991)
263	3-hydroxy-3-methylgutaryl CoA synthase	28304	1652.2	4.86	1263.3	7642	immunologic (Anderson et al., Electrophoresis, 1991)
295	3-hydroxy-3-methylgutaryl CoA synthase	28834	1627.8	4.76	1183.2	5156	immunologic (Anderson et al., Electrophoresis, 1991)
369	3-hydroxy-3-methylgutaryl CoA synthase	54302	855.5	5.70	1849.4	6143	immunologic (Anderson et al., Electrophoresis, 1991)
48	actin (beta)	42857	1118.1	5.05	1406.3	97553	homologous position (Anderson et al., Electrophoresis, 1991)
78	actin (gamma)	42971	1114.9	5.09	1433.5	28391	homologous position (Anderson et al., Electrophoresis, 1991)
296	alpha-2u globulin	19121	2138.3	5.48	1702.7	58948	homologous position (Anderson et al., Electrophoresis, 1991)
668	apolipoprotein A-I	24745	1826.1	5.32	1594.6	3579	homologous position (Anderson et al., Electrophoresis, 1991)
1545	apolipoprotein A-I	24326	1847.8	5.46	1693.7	11349	homologous position (Anderson et al., Electrophoresis, 1991)
52	ATPase F1 alpha (Mitcon:4)	50602	926.8	6.25	2182.2	125806	homologous position (Pavlica et al., BBA, 1990)
33	ATPase F1 beta (Mitcon:1)	49235	958.4	4.71	1139.2	29263	homologous position (Anderson et al., Electrophoresis, 1991)
152	ATPase F1 beta (Mitcon:1)	49480	953.0	4.81	1218.3	[illegible]	homologous position (Anderson et al., Electrophoresis, 1991)
22	ATPase F1 beta (Mitcon:1)	49184	959.6	4.76	1183.9	136043	homologous position (Anderson et al., Electrophoresis, 1991)
140	calmodulin	17706	2223.7	3.99	117.4	26965	homologous position (Anderson et al., Electrophoresis, 1991)
1532	calmodulin	18246	2190.9	3.99	103.7	14421	homologous position (Anderson et al., Electrophoresis, 1991)
505	calreticulin precursor	63181	713.9	4.23	640.6	3952	immunologic (Anderson et al., Electrophoresis, 1991)
161	calreticulin precursor	61117	743.1	4.23	636.5	7321	immunologic (Anderson et al., Electrophoresis, 1991)
2	calreticulin precursor	66594	669.8	4.23	642.2	81703	immunologic (Anderson et al., Electrophoresis, 1991)
51	calreticulin precursor	68951	642.1	4.23	642.0	15293	immunologic (Anderson et al., Electrophoresis, 1991)
58	carbamoyl phosphate synthase	163645	229.4	6.13	2110.0	1397	homologous position (Anderson et al., Electrophoresis, 1991)
394	carbamoyl phosphate synthase	165691	225.9	6.00	2032.2	3350	homologous position (Anderson et al., Electrophoresis, 1991)
139	carbamoyl phosphate synthase	165203	227.0	6.07	2075.7	6488	homologous position (Anderson et al., Electrophoresis, 1991)
10	carbamoyl phosphate synthase	162948	230.6	6.19	2145.6	2416	homologous position (Anderson et al., Electrophoresis, 1991)
7	carbamoyl phosphate synthase	161027	233.7	6.53	2347.0	160715	homologous position (Anderson et al., Electrophoresis, 1991)
0	carbamoyl phosphate synthase	161516	232.9	6.39	2263.0	120304	homologous position (Anderson et al., Electrophoresis, 1991)
3	carbamoyl phosphate synthase precursor	162068	232.0	6.29	2205.0	146476	homologous position (Anderson et al., Electrophoresis, 1991)
11	carbamoyl phosphate synthase precursor	160522	234.6	6.45	2298.7	15435	homologous position (Anderson et al., Electrophoresis, 1991)
67	catalase	58825	778.0	7.48	2868.5	111874	comigration of purified form (Molec. Anat. Lab.)
75	catalase	59152	772.8	7.68	2974.9	89018	comigration of purified form (Molec. Anat. Lab.)
96	cytochrome b5	17326	2247.3	4.57	1009.8	92948	homologous position (Anderson et al., Electrophoresis, 1991)
374	cytochrome b5	17321	2247.6	4.48	922.8	8499	homologous position (Anderson et al., Electrophoresis, 1991)
309	fatty acid binding protein	14780	2409.4	6.90	2552.5	67573	immunologic (Molec. Anat. Lab. via ab from Vanden Heuvel)
28	Grp75 (Mitcon:3)	69196	639.3	5.25	1547.5	16017	immunologic (Mol. Anat. Lab via ab from StressGen)
108	Grp75 (Mitcon:3)	69336	637.8	5.18	1486.1	3398	immunologic (Mol. Anat. Lab via ab from StressGen)
19	Grp75 (Mitcon:3)	69070	640.8	5.36	1623.4	48734	immunologic (Mol. Anat. Lab via ab from StressGen)
116	Grp75 (Mitcon:3)	70868	621.0	5.36	1623.2	6664	immunologic (Mol. Anat. Lab via ab from StressGen)
18	Grp78/BiP	71751	611.7	4.74	1167.3	28304	immunologic (Witzmann et al., Fund. Appl. Tox., 1994)
14	Grp78/BiP	71465	614.7	4.77	1189.5	42583	immunologic (Witzmann et al., Fund. Appl. Tox., 1994)
1537	Grp78/BiP	72356	605.5	4.69	1119.7	647	immunologic (Witzmann et al., Fund. Appl. Tox., 1994)
1536	Grp78/BiP	72076	608.4	4.72	1142.2	5987	immunologic (Witzmann et al., Fund. Appl. Tox., 1994)
5	Grp78/BiP	70965	620.0	4.80	1214.3	64302	immunologic (Witzmann et al., Fund. Appl. Tox., 1994)
4	Grp94 (endoplasmin)	105085	385.2	4.61	1053.4	15428	immunologic (Mol. Anat. Lab via ab from StressGen)
1	Grp94 (endoplasmin)	103957	390.2	4.58	1021.7	57834	immunologic (Mol. Anat. Lab via ab from StressGen)
20	Hsp60 (Mitcon:2)	55968	825.5	5.22	1527.9	114297	immunologic (Mol. Anat. Lab via ab from StressGen)
50	Hsp60 (Mitcon:2)	56396	818.1	5.07	1419.5	7549	immunologic (Mol. Anat. Lab via ab from StressGen)
26	Hsp60 (Mitcon:2)	56222	821.1	5.13	1465.5	40809	immunologic (Mol. Anat. Lab via ab from StressGen)
123	Hsp70	66940	665.6	5.30	1582.9	7606	immunologic (xreact with antiHsp70 from StressGen)
130	Hsp73 (Hsc73) constitutive in unstressed	67475	659.2	5.04	1401.8	4713	immunologic (xreact with antiHsp70 from StressGen)
9	Hsp73 (Hsc73) constitutive in unstressed	68981	645.1	5.14	1474.0	89645	immunologic (xreact with antiHsp70 from StressGen)
24	Hsp73 (Hsc73) constitutive in unstressed	67215	662.3	5.09	1433.5	31112	immunologic (xreact with antiHsp70 from StressGen)
55	Hsp90	85613	493.3	4.72	1149.6	9042	immunologic (Mol. Anat. Lab via ab from StressGen)
12	Hsp90	85291	495.5	4.79	1202.3	25459	immunologic (Mol. Anat. Lab via ab from StressGen)
32	Hsp90	84777	499.2	4.75	1167.6	14525	immunologic (Mol. Anat. Lab via ab from StressGen)
299	lamin B	66121	675.7	4.93	1318.6	2205	homologous position (Anderson et al., Electrophoresis, 1991)
185	lamin B	66260	674.0	4.98	1352.4	3330	homologous position (Anderson et al., Electrophoresis, 1991)
76	laminin receptor protein	42585	1125.6	4.57	1015.6	22461	sequence from gel spot (Meheus, Innogenetics)
351	NADPH cytochrome P450 reductase	72213	607.0	5.13	1467.1	5472	homologous position (Anderson et al., Electrophoresis, 1991)
122	NADPH cytochrome P450 reductase	72216	606.9	5.17	1494.6	10430	homologous position (Anderson et al., Electrophoresis, 1991)
158	pro-albumin	65636	681.7	6.39	2262.0	9377	homologous position (Anderson et al., Electrophoresis, 1991)
74	pro-albumin	65991	677.3	6.50	2327.9	59034	homologous position (Anderson et al., Electrophoresis, 1991)
40	protein disulfide isomerase	53885	863.2	4.59	1030.2	26170	immunologic (Mol. Anat. Lab via ab from StressGen)
15	protein disulfide isomerase	53830	864.3	4.61	1053.6	67905	immunologic (Mol. Anat. Lab via ab from StressGen)
42	protein disulfide isomerase	53661	867.5	4.64	1077.5	17373	immunologic (Mol. Anat. Lab via ab from StressGen)
112	protein disulfide isomerase	53977	861.5	4.57	1014.5	7257	immunologic (Mol. Anat. Lab via ab from StressGen)
275	protein disulfide isomerase	55117	840.6	4.61	1048.4	21670	immunologic (Mol. Anat. Lab via ab from StressGen)
330	pyruvic acid carboxylase	129339	301.2	6.33	2229.8	1782	homologous position (Anderson et al., Electrophoresis, 1991)
111	pyruvic acid carboxylase	129379	[illegible]	6.45	2297.0	12435	homologous position (Anderson et al., Electrophoresis, 1991)
43	pyruvic acid carboxylase	128864	5	6.38	2258.9	3991	homologous position (Anderson et al., Electrophoresis, 1991)
186	pyruvic acid carboxylase	129556	300.6	6.52	2337.3	7735	homologous position (Anderson et al., Electrophoresis, 1991)
141	senescence marker protein (SMP30)	35546	1353.0	4.85	1256.6	23626	sequence from gel spot (Meheus, Innogenetics)
62	senescence marker protein (SMP30)	35560	1352.5	4.97	1346.0	111435	sequence from gel spot (Meheus, Innogenetics)
45	serum albumin precursor	65731	680.5	6.10	2094.5	59197	homologous position (Anderson et al., Electrophoresis, 1991)
508	serum albumin precursor	65699	680.9	5.97	2016.3	10356	homologous position (Anderson et al., Electrophoresis, 1991)
187	superoxide dismutase	16823	2278.6	6.13	2111.7	143464	homologous position (Anderson et al., Electrophoresis, 1991)
287	superoxide dismutase	36308	1325.6	6.78	2476.1	37004	homologous position (Anderson et al., Electrophoresis, 1991)
391	tubulin alpha	53180	876.7	4.88	1275.0	7388	homologous position (Anderson et al., Electrophoresis, 1991)
60	tubulin alpha	54317	855.2	4.96	1264.1	14328	homologous position (Anderson et al., Electrophoresis, 1991)
124	tubulin alpha	53879	863.3	4.88	1279.0	13252	homologous position (Anderson et al., Electrophoresis, 1991)
494	tubulin alpha	54197	857.4	4.84	1244.0	6261	homologous position (Anderson et al., Electrophoresis, 1991)
29	tubulin beta	53942	862.2	4.75	1170.0	30411	homologous position (Anderson et al., Electrophoresis, 1991)

FIGURE 21

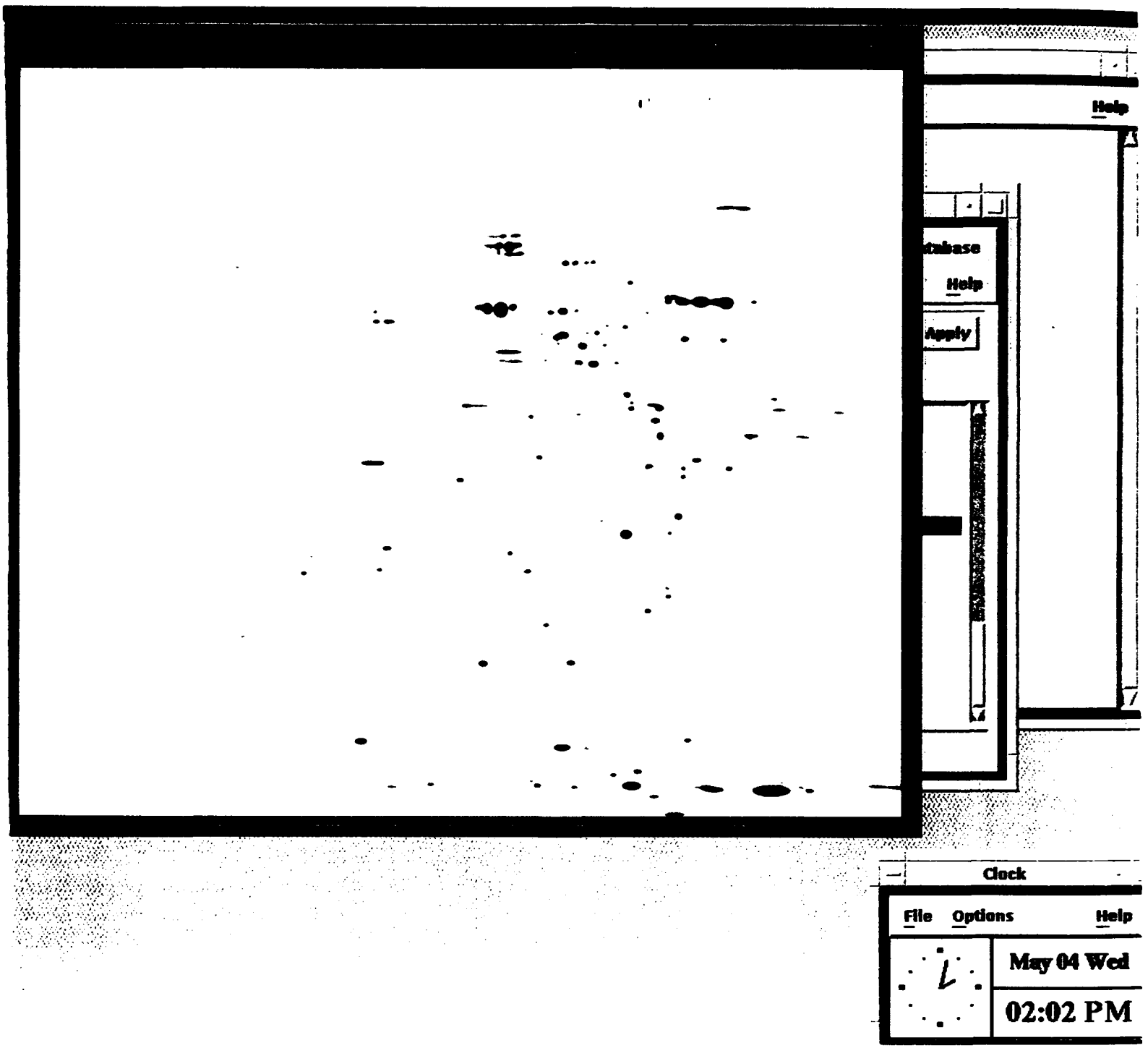

ADDENDUM B

MALDI Peptide-mass Determination:

Bovine Hemoglobin-alpha

MSMW	MOWSE	SEQ	AA
2980	2970	LLSHSLLVTLASHLPSDFTPAVHASLDK	100-127
2376	2368	AVEHLDDLPGALSELSDLHAHK	69-90
1840	1834	TYFPHFDLSHGSAQVK	41-56
1534	1530	VGGHAAEYGAEALER	17-31
1276	1279	FLANVSTVLTSK	128-139

Bovine Hemoglobin-beta

MSMW	MOWSE	SEQ	AA
2098	2090	FFESFGDLSTADAVMNNPK	40-58
1427	1423	EFTPVLQADFQK	120-131
1276	1275	LLVVYPWTQR	30-39
1182	1177	VVAGVANALAHR	132-143
1092	1097	VLDSFSNGMK	66-75
952	950	AAVTAFWGK	8-16

```
    #3          23-SEP-1993 09:25:00.34
NEWMAIL
From:    IN%"mowse@dl.ac.uk"
To:      IN%"lsbcorp@delphi.com"
CC:
Subj:

Return-path: <mowse@dl.ac.uk>
Received: from mserv1.dl.ac.uk by delphi.com (PMDF V4.2-11 #4520) id
 <01H3A6YYSTN49877BV@delphi.com>; Thu, 23 Sep 1993 09:24:52 EDT
Received: from s-ind2 (s-ind2.dl.ac.uk) by mserv1.dl.ac.uk with SMTP id
AA13246
 (5.65c/DL-V3.2.1(DNS-IDE-pg) for <lsbcorp@biotechnet.com>  from
 mowse@dl.ac.uk); Thu, 23 Sep 1993 14:18:03 +0100
Received: by s-ind2 (920330.SGI/930727.MJE) for lsbcorp@biotechnet.com id
 AA12309; Thu, 23 Sep 93 15:27:12 +0100
Date: Thu, 23 Sep 1993 15:27:12 +0100
From: mowse@dl.ac.uk (Mowse Server)
To: lsbcorp@delphi.com
Message-id: <9309231427.AA12309@s-ind2>
Content-transfer-encoding: 7BIT
Precedence: first-class
Database: /nfs/fab1/data2/owl/owl
Reagent: Trypsin
Tolerance: 10 dalton
Apparently-To: lsbcorp@biotechnet.com

Sequence MW: 15200
MW filter: 30%


SCAN of /nfs/fab1/data2/owl/owl using reagent Trypsin
USING fragment mws of:
          4244
          2980
          2376
          2098
          1840
          1534
          1482
          1427
          1276
          1182
          1092
          952
          805
          618
          442
No. of hits = 30 (MAX. ALLOWED)
No. of database entries scanned = 65895
1   . HBA_BOVIN     HEMOGLOBIN ALPHA CHAIN. - BOS TAURUS (BOVINE).
2   . JS0680        hypothetical protein 3 (gldA 5' region) - Bacillus
stearotherm
3   . VAL3_TGMV     AL3 PROTEIN. - TOMATO GOLDEN MOSAIC VIRUS (TGMV).
4   . X_HPBVY       PROTEIN X. - HEPATITIS B VIRUS (SUBTYPE AYW).
5   . HBB_BOVIN     HEMOGLOBIN BETA CHAIN. - BOS TAURUS (BOVINE).
6   . HBBA_BOSJA    HEMOGLOBIN BETA-A CHAIN. - BOS JAVANICUS (WILD BANTENG).
7   . HBB_BOSGA     HEMOGLOBIN BETA CHAIN. - BOS GAURUS FRONTALIS (GAYAL).
8   . PHA1_SYNPY    C-PHYCOERYTHRIN CLASS I ALPHA CHAIN. - SYNECHOCOCCUS SP.
(STRA
9   . HBE_RABIT     HEMOGLOBIN EPSILON CHAIN (BETA-4). - ORYCTOLAGUS CUNICULUS
(RA
10  . HBA1_BOSMU    HEMOGLOBIN ALPHA-1 CHAIN. - BOS MUTUS GRUNNIENS (YAK).
```

```
11 . S14886        Hypothetical protein 9 - Yeast (Hansenula polymorpha)
12 . JT0902        chaperonin 60 beta - wheat (fragment)
13 . HBA_RANTA     HEMOGLOBIN ALPHA CHAIN. - RANGIFER TARANDUS (REINDEER).
14 . HBG_LEMFU     HEMOGLOBIN GAMMA CHAIN. - LEMUR FULVUS FULVUS (BROWN
LEMUR).
15 . S29555        Chalcone isomerase (EC 5.5.1.6) - Apple tree (fragment)
16 . S29554        Chalcone isomerase (EC 5.5.1.6) - Apple tree (fragment)
17 . YZFB_ECOLI    VERY HYPOTHETICAL 18.0 KD PROTEIN IN FEPB 3'REGION. -
ESCHERIC
18 . HBA2_BOSMU    HEMOGLOBIN ALPHA-2 CHAIN. - BOS MUTUS GRUNNIENS (YAK).
19 . PL0018        Ig heavy chain V-D-J region (RP93) - mouse (fragment)
20 . S03527        Ig heavy chain V region - African clawed frog
21 . LGB_PSOTE     LEGHEMOGLOBIN. - PSOPHOCARPUS TETRAGONOLOBUS (GOA BEAN)
(ASPAR
22 . S24697        Ig heavy chain V6 region - Human
23 . PHEA_PORCR    B-PHYCOERYTHRIN ALPHA CHAIN. - PORPHYRIDIUM CRUENTUM.
24 . PHEA_PORSO    B-PHYCOERYTHRIN ALPHA CHAIN. - PORPHYRIDIUM SORDIDUM.
25 . CBPA_PIG      CARBOXYPEPTIDASE A (EC 3.4.17.1) (FRAGMENT). - SUS SCROFA
(PIG
26 . CEUIFN        CEUIFN LOCUS CEUIFN 501 bp ss-mRNA MAM 07-DEC-1992 - Cervus
el
27 . HBB_LAMGL     HEMOGLOBIN BETA CHAIN. - LAMA GLAMA (LLAMA), LAMA VICUGNA
(VIC
28 . HBB_CAMDR     HEMOGLOBIN BETA CHAIN. - CAMELUS DROMEDARIUS (DROMEDARY)
(ARAB
29 . S41176        S41176 transactivator; For the protein sequence (NCBI
gibbsq
1
30 . S41175        S41175 transactivator; For the protein sequence (NCBI
gibbsq
1

    1  : HBA_BOVIN       2.893509e+05 15053       0.333
         HEMOGLOBIN ALPHA CHAIN. - BOS TAURUS (BOVINE).
         MW      START  END     SEQ
         4244    NO MATCH
         2970    100    127     LLSHSLLVTLASHLPSDFTPAVHASLDK
         2368    69     90      AVEHLDDLPGALSELSDLHAHK
         2098    NO MATCH
         1834    41     56      TYFPHFDLSHGSAQVK
         1530    17     31      VGGHAAEYGAEALER
         1482    NO MATCH
         1427    NO MATCH
         1279    128    139     FLANVSTVLTSK
         1182    NO MATCH
         1092    NO MATCH
         952     NO MATCH
         805     NO MATCH
         618     NO MATCH
         442     NO MATCH

    2  : JS0680          1.699716e+05 18173       0.333
         hypothetical protein 3 (gldA 5' region) - Bacillus
stearothermophilus
         MW      START  END     SEQ
         4253    48     81      AGLDYWEFVNIHYYDSLDHFFQQNQNGDFYYITK
         2980    NO MATCH
         2376    NO MATCH
         2098    NO MATCH
         1832    133    149     ALNLSNTAAILVYEALR
         1534    NO MATCH
         1473    86     97      YYTSYDFSDPSK
         1427    NO MATCH
```

1276	NO MATCH		
1182	NO MATCH		
1088	113	121	ELLAENEDR
959	125	132	IPMTENVR
805	NO MATCH		
618	NO MATCH		
442	NO MATCH		

5 : HBB_BOVIN 5.948711e+04 15954 0.400
HEMOGLOBIN BETA CHAIN. - BOS TAURUS (BOVINE).

MW	START	END	SEQ
4244	NO MATCH		
2980	NO MATCH		
2376	NO MATCH		
2090	40	58	FFESFGDLSTADAVMNNPK
1840	NO MATCH		
1534	NO MATCH		
1482	NO MATCH		
1423	120	131	EFTPVLQADFQK
1275	30	39	LLVVYPWTQR
1177	132	143	VVAGVANALAHR
1097	66	75	VLDSFSNGMK
950	8	16	AAVTAFWGK
805	NO MATCH		
618	NO MATCH		
442	NO MATCH		

6 : HBBA_BOSJA 5.944985e+04 15964 0.400
HEMOGLOBIN BETA-A CHAIN. - BOS JAVANICUS (WILD BANTENG).

MW	START	END	SEQ
4244	NO MATCH		
2980	NO MATCH		
2376	NO MATCH		
2090	40	58	FFESFGDLSTADAVMNNPK
1840	NO MATCH		
1534	NO MATCH		
1482	NO MATCH		
1423	120	131	EFTPVLQADFQK
1275	30	39	LLVVYPWTQR
1177	132	143	VVAGVANALAHR
1098	66	75	VLDSFSDGMK
950	8	16	AAVTAFWGK
805	NO MATCH		
618	NO MATCH		
442	NO MATCH		

7 : HBB_BOSGA 5.936803e+04 15986 0.400
HEMOGLOBIN BETA CHAIN. - BOS GAURUS FRONTALIS (GAYAL).

MW	START	END	SEQ
4244	NO MATCH		
2980	NO MATCH		
2376	NO MATCH		
2090	40	58	FFESFGDLSTADAVMNNPK
1840	NO MATCH		
1534	NO MATCH		
1482	NO MATCH		
1423	120	131	EFTPVLQADFQK
1275	30	39	LLVVYPWTQR
1177	132	143	VVAGVANALAHR
1097	66	75	VLDSFSNGMK
950	8	16	AAVTAFWGK
805	NO MATCH		